

Genetic components of root architecture and anatomy adjustments to water-deficit stress in spring barley

Benedict C. Oyiga¹  | Janina Palczak¹ | Tobias Wojciechowski² | Jonathan P. Lynch³  | Ali A Naz¹ | Jens Léon¹ | Agim Ballvora¹

¹INRES-Plant Breeding, University of Bonn, Bonn, Germany

²Forschungszentrum Jülich, Institute for Bio- and Geosciences (Plant Sciences), Bonn, Germany

³Department of Plant Science, The Pennsylvania State, State College, Pennsylvania

Correspondence

A Ballvora, INRES-Plant Breeding, University of Bonn, Bonn, Germany
Email: ballvora@uni-bonn.de

Funding information

Deutsche Forschungsgemeinschaft e.V. (DFG) and Institute of Bio- and Geosciences, Plant Sciences (IBG-2), Jülich., Grant/Award Number: PAK 770

Abstract

Roots perform vital roles for adaptation and productivity under water-deficit stress, even though their specific functions are poorly understood. In this study, the genetic control of the nodal-root architectural and anatomical response to water deficit were investigated among diverse spring barley accessions. Water deficit induced substantial variations in the nodal root traits. The cortical, stele, and total root cross-sectional areas of the main-shoot nodal roots decreased under water deficit, but increased in the tiller nodal roots. Root xylem density and arrested nodal roots increased under water deficit, with the formation of root suberization/lignification and large cortical aerenchyma. Genome-wide association study implicated 11 QTL intervals in the architectural and anatomical nodal root response to water deficit. Among them, three and four QTL intervals had strong effects across seasons and on both root architectural and anatomical traits, respectively. Genome-wide epistasis analysis revealed 44 epistatically interacting SNP loci. Further analyses showed that these QTL intervals contain important candidate genes, including *ZIFL2*, *MATE*, and *PPIB*, whose functions are shown to be related to the root adaptive response to water deprivation in plants. These results give novel insight into the genetic architectures of barley nodal root response to soil water deficit stress in the fields, and thus offer useful resources for root-targeted marker-assisted selection.

KEYWORDS

Barley (*Hordeum vulgare*), Epistatic QTL pairs, Genome-wide association study, Nodal root anatomical traits, Nodal root architecture, Water-deficit stress

1 | INTRODUCTION

Water-deficit stress induces osmotic and oxidative stresses in plants (Ahanger et al., 2014). It affects plants at morphological (e.g., reduced germination vigor, plant biomass, and various root traits), physiological

(e.g., reduced photosystem II activity, stomatal conductance, membrane stability, and abscisic acid content), biochemical (e.g., accumulation of proline, sugars, phytohormones, and antioxidants), and molecular (e.g., alteration of expression of defense/stress-related genes) levels; subsequently affecting crop yield. Three approaches exist to minimize the negative impact of water stress on crops: (a) conserve soil water, (b) access more water, and (c) overcome special water-deficit sensitivities (Sadok,

Benedict C. Oyiga and Janina Palczak authors contributed equally to this work.

This is an open access article under the terms of the Creative Commons Attribution License, which permits use, distribution and reproduction in any medium, provided the original work is properly cited.

© 2019 The Authors. Plant, Cell & Environment published by John Wiley & Sons Ltd

and Sinclair, 2011). Studies indicate that roots play a crucial role in water-stress perception (Janiak et al., 2015; Ksouri et al., 2016), water acquisition (Ehdaie et al., 2012; Palta and Yang, 2014; Lynch et al., 2014; Paez-Garcia et al., 2015), as well as adaptation and tolerance to water-deficit stress (Geng et al., 2018). Considerable variation in root traits that are regulated by multiple genes have been observed in many crop species (Steele et al., 2007; Bernier et al., 2009; Manavalan et al., 2012; Pacheco-Villalobos and Hardtke, 2012), indicating that water-stress adaptation and yield in crops can be improved via selection for root traits in breeding programs.

Crops with deeper and thinner root systems are more favorably adapted to soils undergoing scenarios of water-deficit stress than those with shallow and thick rooting systems (Ram, 2014; Lynch, 2014). Important root traits for water-stress adaptation include: greater primary root elongation, deeper root systems, suppression of the lateral root branching, redistribution of branch root density from surface to depth, and elongation of root hairs (Jovanovic et al., 2007; Wasson et al., 2012; Uga et al., 2013; Lynch, 2013; Lynch et al., 2014; Smith and De Smet, 2012; Comas et al., 2013). These traits may be controlled by several molecular networks (Kulkarni et al., 2017) that regulate gene expression and induce the accumulation of stress proteins to modulate plant-water balance. The suppression of root growth after initiation (arrested roots) has been observed in plants under water-deficit stress (Xiong, Li, & Zhang, 2006; Xiong, Wang, Mao, & Koczan, 2006; Sebastian et al., 2016; Zhan et al., 2015).

Despite the critical and adaptive roles of roots (Tuberosa et al., 2003; Lynch, 2007; Tron et al., 2015), our understanding of their genetic basis of adaptations against water-deficit stress is poor, in part because of the challenge of root phenotyping in the field (Wasson et al., 2012; Topp et al., 2013; Burton et al., 2015; Khan et al., 2016; Merchuk-Ovnat et al., 2017) and the uncertainty about which traits to target. Root system characteristics, including elongation, growth angle, and branching pattern/density, are determined by genetic and environmental factors (Lynch and Brown, 2012). The evaluation of desirable root traits would enhance the dissection of root adaptive response to water-deficit stress. Thus, would facilitate the development of high-yielding and water-deficit stress resilient cultivars that are capable of accessing water in deeper soil layers. The genetics of root adaptations to water deficit involves the integration of several aspects of root biology and models that analyze the root morpho-anatomical changes. Selecting genotypes with appropriate root architecture may increase yields (Lynch and Beebe, 1995). Lynch (2013) and Lynch and Wojciechowski (2015) have proposed using root architectural and anatomical traits to accelerate understanding of the root subsoil water exploration and acquisition in plants. The emergence of DNA-markers, efforts to sequence the whole barley genome, and the availability of powerful biometric methods have made the identification of quantitative trait loci (QTL)/genes associated with yield and water-stress tolerance possible. These water stress-related QTL can be used as markers in breeding programs for developing drought-tolerant (Farooq et al., 2009, 2010; Ashraf, 2010) and high-yielding genotypes.

Genome-wide association study (GWAS) based on linkage disequilibrium (LD) has been applied in crops to dissect the genetic and molecular basis of several highly complex quantitative traits (Jighly et al., 2015; Contreras-Soto et al., 2017; Fang et al., 2017; Oyiga et al., 2018, 2019;

Ogbonnaya et al., 2017; Thoen et al., 2017). Decades of research have led to the uncovering of genes involved in root growth and development, such as *Deeper Rooting 1* (Uga et al., 2013; Arai-Sanoh et al., 2014), *Retarded Root Growth* (Zhou et al., 2011), *Roothairless5* (Nestler et al., 2014), *Root Systems Architecture 1* (Rosas et al., 2013), and *Crown Rootless1* (Coudert et al., 2015). However, most of these studies were performed in the genetic backgrounds of plants such as *Arabidopsis* and tropical cereals such as rice, and maize, but not in temperate cereals such as barley and wheat. Moreover, few studies have analyzed the genetic control of the nodal root architectural and anatomical changes during episodes of soil water shortages via GWAS in plant species (Zaidi et al., 2016; Kadam et al., 2017); but none has so far been performed in barley to elucidate for these components, which could act as a model for other temperate cereals.

This study aims to explore the phenotypic variation existing among 192 diverse barley genotypes to identify QTL involved in both additive and epistatic effects of architectural and anatomical nodal root response against soil water deprivation stress in barley and to provide insights into their genetic control. This study provides an important useful resource for undertaking further fine mapping studies, and finally, proof-of-function of the causative genes.

2 | MATERIALS AND METHODS

2.1 | Plant material

The plant material used in this study consists of 192 genotypes of a barley diversity panel. They were constructed from the barley core collection and the barley gene bank collection at IPK Gatersleben, Germany, including 111 two-rowed and 81 six-rowed spring barleys originating from Europe and Russia (96), West Asia and North Africa (36), South and East Asia (33), and United States (27). Among them, 129, 47, and 16 are old/new cultivars, landraces, and breeding materials, respectively (Table S1).

2.2 | Field evaluation trials

The field evaluations were conducted in 2013, 2014, and 2015 at Campus Klein-Altendorf Research Facility (50°37' N, 6°59' E), University of Bonn, Germany, under rainfed (control) and water-deficit stress (rain-out shelter) conditions. The rain-out shelter is made up of an electrical motorized system for rolling part of the roof cover. The roof cover opens to equilibrate with the external ambient conditions and closes during rainfall to exclude rain water. In both control and water-deficit conditions, the GWAS panel was grown in a lattice square design of 0.8 m long rows and 0.21 m between row plot size. The plots were irrigated by moveable overhead sprinklers which were programmed to deliver ~5.00 mm/day water per day. Water stress was introduced by withholding water to the plants at BBCH20 (tiller-initiation stage) and continued until data collection at heading (BBCH51). All plots were maintained by adopting all standard agronomic practices. The root architectural and

anatomical traits were collected from two (in 2013) and three (in 2014 and 2015) replicates per genotype in control and water-deficit stress conditions. Figure S1 shows the soil moisture content (0–30 cm) of the experimental plots in 2013, 2014, and 2015 under control and water-deficit stress conditions.

2.3 | Phenotyping root architecture (morphology) by “Shovelomics”

The diversity panel was root phenotyped by “Shovelomics” (Trachsel et al., 2011). In brief, genotypes at BBCH51 (in control and water-stressed plots) were excavated with a shovel at a distance of ~0.2 m away from the plant base to avoid root destruction. The lumps of excavated soil containing the roots were dissolved by submerging in a bucket of fresh water for ~5 min. Thereafter, roots were gently washed to remove the remaining soil debris and rinsed with clean water. The nodal root growth angles of roots from the main shoots and tillers were measured by (a) placing clean roots on a phenotyping board fitted with a large protractor (2013) and (b) taken to the imaging station “field photo box” for photo-image acquisition (2014 and 2015). In both cases, root growth angles were determined by measuring the angle between the soil surface (horizontal line) and the shallowest nodal roots. Since water-deficit stress inhibits root growth after initiation, the number of nodal and stagnated/arrested nodal roots were obtained by counting from the main shoot and tillers under control and water-deficit conditions.

2.4 | Phenotyping of root anatomical traits using laser ablation tomography (LAT)

To investigate the impact of water-deficit stress on the nodal root anatomy, sections (1–2 cm length) of nodal roots ablated from the main-shoot and tillers at a position 1 cm from the root base were obtained: two (in 2013) and three (2014 and 2015) replicates for each genotype/treatment. The harvested root sections were immediately placed in Eppendorf safe-lock tubes containing 75% ethanol for preservation until analysis. Anatomical images were obtained from the root segments *via* ablation using LAT (Chimungu et al., 2014, 2015; Strock et al., 2019; Hall and Lanba, 2019) at Penn State University. LAT is a semi-automated system that uses a pulsed laser beam (Avia 7000, 355 nm pulsed laser) to ablate root tissue at the camera focal plane ahead of an imaging stage. Here, the root samples were incrementally extended into the beam, vaporized or sublimated, and imaged simultaneously using a Canon T3i camera (Canon Inc. Tokyo, Japan) and 5× micro lens (MP-E 65 mm) on the laser-illuminated surface. The root images obtained were analyzed using *RootScan*, an image-analysis tool developed for analyzing root anatomy (Burton et al., 2012). The primary and secondary anatomical root traits obtained *via* pixel counting (in square millimeters) in control and water-deficit stress conditions include (Table 1): *mCRA*, *mRXSA*, *mXVA*, *mTSA*, *mNXV*, *tNXV*, *tCRA*, *tRXSA*, *tTSA*, *tXVA*, *mAXVA*, *tAXVA*, *mXVA/mRXSA*, and *tXVA/tRXSA*.

2.5 | Statistical analyses of the phenotypic traits

Year-specific analyses of variance (ANOVA) were performed on the replicated root data obtained using restricted maximum likelihood (REML) model, to investigate the effects of genotypes, water deficit, and their interactions across seasons. Effects due to planting positions (row-and-column effects) in the field plots were accounted for by including “Replication/Row*Column” (Gilmour Thompson, & Cullis, 1995): rows crossed with columns nested within replication in the REML as random effects; whereas, the genotype and water-deficit stress treatment effects were considered to be fixed. Significant differences ($P \leq .05$) among genotypes, between water-deficit stress treatments, and their interactions were determined using WALT statistics. The best linear unbiased estimates

TABLE 1 Description of root morphological and anatomical traits evaluated in this study

	Root Traits	Description
Root Architectural Nodal Root Traits		
1.	mANR	Number of arrested nodal roots of the main shoot axis
2.	tANR	Number of arrested nodal roots of the tiller
3.	TwNR	Number of tiller with nodal roots
4.	TwANR	Number of tiller with arrested nodal roots
5.	mNRpP	Number of nodal roots emerged at the main shoot axis
6.	tNRpP	Number of nodal roots emerged at the tiller
7.	mRGA	Main shoot nodal root growth angle
8.	tRGA	Tiller nodal root growth angle
Root Anatomical Nodal Root Traits		
9.	mRXSA	Main shoot nodal root cross sectional area (mm ²)
10.	mTSA	Main shoot nodal root stele area (mm ²)
11.	mCRA	Main shoot axis nodal root cortical area (mm ²) = mRXSA – mTSA
12.	mXVA	Main shoot nodal root xylem vessel area (mm ²)
13.	mAXVA	Average area of the main shoot nodal root xylem vessel (mm ²)
14.	mXVA/mRXSA	Main shoot nodal root xylem vessel area to cross sectional area ratio
15.	mNXV	Number of main shoot nodal root xylem vessels
16.	tRXSA	Tiller nodal root cross sectional area (mm ²)
17.	tTSA	Tiller nodal root stele area (mm ²)
18.	tCRA	Tiller nodal root cortical area (mm ²) = tRXSA – tTSA
19.	tXVA	Tiller nodal root xylem vessel area (mm ²)
20.	tAXVA	Average area of the tiller nodal root xylem vessel (mm ²)
21.	tXVA/tRXSA	Tiller nodal root xylem vessel area to cross sectional area ratio
22.	tNXV	Number of tiller nodal root xylem vessels

(BLUEs) of the nodal root traits were obtained using GenStat 16 (GenStat, 2014). The BLUEs were used to calculate the root drought tolerance indices (DTI) as: $Y_p * Y_s / (\bar{Y}_p)^2$ (Fernandez, 1992), where Y_p = BLUEs of genotypes under control, Y_s = BLUEs of genotypes under water deficit, and \bar{Y}_p = mean BLUEs of genotypes under the control. DTI index is suitable for discriminating genotypes on the basis of drought tolerance status and yield potential (Fernandez, 1992; Sio-SeMardeh, Ahmadi, Poustini, & Mohammadi, 2006; Mohammadi et al., 2010). The broad-sense heritability (H^2) of the traits were also calculated as a ratio of the components of genetic and phenotypic variances, as implemented in GENSTAT 16 for REML (O'Neill, 2010). Pearson correlation and summary statistics were obtained for the traits genotypic means using SPSS software (SPSS version-16, Inc, Chicago, IL, USA).

2.6 | Genotyping of the barley diversity panel

The diversity panel was genotyped with 9K iSELECT SNP chip (Jia et al., 2019) and genotyping-by-sequencing (GBS) assays. The DNA was extracted from seedlings at the two-leaf stage as described by Stein et al. (2001). Thereafter, the GBS analysis and enzymatic digestion were performed and after library preparation the enriched DNA fragments were pair end sequenced using NGS technology *PstI* (manuscript in preparation). All GBS SNP markers were aligned against the reference barley genome sequence "150831 barley pseudomolecules.fasta" (Mascher et al., 2017). Prior to the genetic analyses, SNP markers with allele frequency ≤ 0.05 and call rate ≤ 0.9 were excluded. Thus, 8,987 DNA-polymorphic markers across the barley genome comprising 6335 iSELECT and 2652 GBS SNP markers were used for the GWAS.

2.7 | Population structure and linkage disequilibrium (LD) analysis

The population structure of the panel was analyzed based on a Bayesian clustering method as implemented in STRUCTURE v.2.3.4 (Pritchard et al., 2000) using 785 unlinked markers (MAF > 5%; <2% missing data and spaced approximately 2 cM apart). The admixture model was applied with no previous population information. The number of subpopulation (K) tested ranged from 1 to 9, with 20 replications per K . The burn-in period and the number of Markov chain Monte Carlo (MCMC) iterations were 1000,000 and 1000,000, respectively. Number of K was determined following the procedure described by Evanno et al. (2005). Thereafter, we plotted the genetic relationships among the genotypes via principal coordinates analysis (PCoA) in GenAIEx 6.5 (Peakall & Smouse, 2012). The pairwise LD was calculated with 6,272 SNPs (with known genetic position) as implemented in TASSEL 5.0 (Bradbury et al., 2007). To investigate the population LD decay rate, the r^2 values obtained for each chromosome were plotted against the genetic distance (cM) between SNP pairs and a cut off of $r^2 = 0.1$ was chosen as the critical distance up to which a gene locus extends.

2.8 | Identification of QTL for barley nodal root responses to water deficit

The QTL associated with changes in the nodal root architectural and anatomical traits due to water-deficit stress were identified using GWAS mixed linear (MLM-PK) approach. Here, the root DTIs were included as phenotype, and the confounding effects of population stratification in the panel was accounted for by including kinship (K-matrix) and population structure (P-matrix) (Price et al., 2010; Kang et al., 2010) as covariates. The K-matrix and P-matrix (principal component analysis) were generated using TASSEL 5.0 (Bradbury et al., 2007). GWAS were performed in TASSEL 5.0, and the results obtained were verified using PROC MIXED macro program. The model used is described as: $y = X\beta + S\alpha + Qv + Zu + e$, where y is the vector of DTIs; β is the fixed effects other than SNP or population structure; α represents the vector of SNP effects; v is the vector of population effects; u is the vector of polygene background effects; α is a vector of SNP effects; v is a vector of population effects; u is a vector of polygene background effects; e is a vector of residual effects; Q is the matrix from STRUCTURE relating y to v ; X , S , Z are incidence matrices (0/1) relating y to β , α , and u , respectively (Yu et al., 2006). The FDR adjusted p -value (q -value) of 0.01 was estimated with Q-VALUE (Storey and Tibshirani, 2003) and used to correct for the multiple testing. Only significant marker-trait associations (MTAs) with q -values below the FDR ≤ 0.01 threshold were reported. All the associated SNPs in high chromosomal LD with each other were considered to be linked (SNP-clusters).

2.9 | Detection of epistatically interacting loci involved in root water stress adaptation

Genome-wide two-locus epistatic interactions were surveyed using the "interactions" function of PROC MIXED procedure in SAS 9.4 (SAS Institute, Cary, NC, USA); by fitting a linear model with $P + K$ variables, the additive effects of the markers and their interactions. The P -value cutoff was set at 1×10^{-6} for both total effects and gene-gene interaction effects. Only loci that met these statistical criteria were examined and reported. The significance threshold was determined by cross validation and 1,000 random permutations. The interaction graph was drawn using Circos 0.63-4 (Krzywinski et al. 2009).

2.10 | Identification of candidate genes in the vicinity of the significant SNP markers

To obtain barley candidate genes involved in the nodal root response to water-deficit stress, BLAST searches were made in the public Barley Genome Gene-set database (BARLEX; <http://apex.ipk-gatersleben.de>) using the core sequences of the significant SNPs. Top gene hits were identified by identity scores of greater than 80% and e -values less than $1e-70$. Because GWAS-identified SNPs may be part of a larger QTL region of correlated genetic variants (van der Sijde et al., 2014), we also searched for other possible gene candidates that

may be located ≤ 5 Mbp up- and down-stream of the significant QTL (de Koning and Haley, 2005; Ge et al., 2009). The searches were performed in the IPK Barley Genome database (https://apex.ipk-gatersleben.de/apex/f?p=284:41:::NO:RP:P41_GENE_CHOICE:2).

Only the annotated high confidence (HC) genes [genes with known annotation and verified position on the WGS assembly of cv. Morex (IBGC., 2012)] were obtained in these expanded QTL regions from the database. Thereafter, candidate genes functioning in the molecular pathways related to root response to water-deficit stress were selected as additional candidate genes.

3 | RESULTS

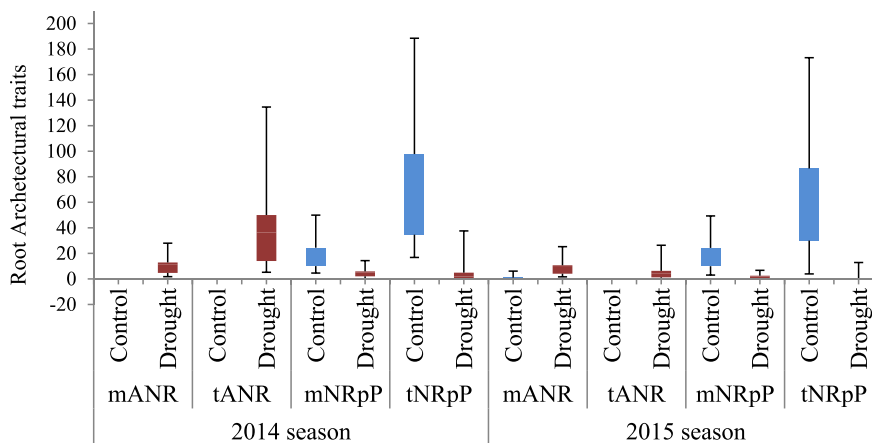
3.1 | Phenotypic diversity of root traits under field-induced water-deficit stress

To evaluate root responses to water shortage, architectural and anatomical traits of nodal roots were analyzed among 192 genotypes of barley panel under control and water-deficit conditions in 2013, 2014, and 2015.

3.1.1 | Nodal root architectural traits

Analysis of variance (ANOVA) performed revealed substantial genotypic variability for nodal root architectural traits (Figure 1; Table 2). Except in a few cases, the effects of water stress and the interactions between genotype and water stress in 2014 and 2015 were significant. Most of the architectural traits exhibited moderate broad-sense heritability ($H^2 = 51.6\text{--}64.9\%$); with the exception of the number of arrested nodal roots in the tillers (tANR) and the number of tillers with arrested nodal roots (TwANR) in 2015. Prolonged periods of water deprivation increased the growth angle of main shoot nodal roots by +5.8 and +2.6% in the 2013 and 2015, respectively. It also increased the number of arrested nodal roots of both main shoot and tillers in 2014 and 2015 (Figure 1).

FIGURE 1 Number of arrested nodal roots at BBCH 51 under control (in blue) and drought stress (in red) conditions in 2014 and 2015 experimental field trials. *mANR*: arrested nodal roots of the main shoot axis; *tANR*: arrested nodal roots of the tiller; *mNRpP*: number of nodal roots emerged at the main shoot axis; *tNRpP*: number of nodal roots emerged at the tiller



3.1.2 | Nodal root anatomical traits

The ANOVA showed that there were significant ($P < .01$) differences among genotypes for anatomical nodal root traits in response to water deficit. Significant water-deficit stress and genotype \times water-deficit stress interactions were also observed in most of the anatomical root traits. Except in a few cases, the H^2 were moderate, ranging from 10.0 to 52.0% (2013) and 9.0 to 37.0% (2014). Prolonged water deficit decreased the total nodal root cortical area (*mCRA*) (-9.57 and -14.63%), root stele area (*mTSA*) (-28 and -4.12%), and cross-sectional root area (*mRXSA*) (-8.22 and -16.94%) of the main shoot in 2013 and 2014, respectively. However, water-deficit stress increased these traits in the tillers—*tCRA* ($+8.03$ and $+11.93\%$), *tTSA* ($+6.56$ and $+1.91\%$), and *tRXSA* ($+7.69$ and $+10.84\%$) in 2013 and 2014, respectively. The mean, coefficients of genetic variation (CV), skewness, and kurtosis of the nodal root anatomical traits are summarized in Table 2. Anatomical nodal root images obtained indicated that the stele cross-sectional area and the number of meta-xylem vessels increased under water-deficit stress (Figure 2). There was an evidence of increased formation of well-defined specialized tissues, such as rhizodermis with thickened outer cell walls as well as well-developed suberized exodermis and endodermal cell layers around the stele of the stressed roots compared to the unstressed ones. Under water-deficit stress, root cortical aerenchyma and root cortical cell size were also substantially increased.

3.1.3 | Nodal root trait drought tolerance indices

Traits DTIs are suitable for discriminating genotypes based on their levels of drought stress tolerance and yield potential and can be exploited to identify QTL associated with the traits of interest. ANOVA results indicate the existence of relatively large genetic variability among the genotypes for the root DTIs (Table 2), with high CV ranging from 12.87 to 87.10%, 12.44 to 76.46%, and 14.38 to 87.10% in 2013, 2014, and 2015, respectively. Repeatability estimates (R) for the evaluated root DTI traits were

TABLE 2 ANOVA and trait drought stress indices summary statistics of root architectural and anatomical traits among a barley diversity panel under field (control) and rain-out shelter (water stress) conditions

Year	Root Traits	Mean squares					E (%)	G	DTI CV	R (%)	Skew	Kur
		G	Dr	G*Dr	H ²	H ²						
Root Architectural Traits												
2013	mRGA	**	**	ns	0.60	+5.82	**	28.17	99.97	-0.08	-0.45	
	tRGA	**	**	ns	0.52	+5.20	**	32.75	99.02	0.04	-0.9	
2014	mANR	**	—	—	0.65	—	**	37.36	99.12	0.77	0.48	
	tANR	**	—	—	0.57	—	**	62.66	99.10	1.09	0.73	
	mNRpP	**	**	ns	0.62	-76.06	**	59.27	99.90	0.98	1.66	
	tNRpP	**	**	**	0.53	-93.44	**	18.50	99.77	3.87	—	
	TwANR	**	—	—	0.52	—	**	13.76	99.00	2.51	7.82	
	TwNR	**	**	*	0.63	-98.01	**	51.94	99.21	1.30	2.74	
2015	mRGA	**	**	**	0.52	+2.57	**	14.38	99.12	-0.57	1.09	
	mANR	**	—	—	0.59	—	**	35.12	99.52	0.97	2.17	
	tANR	ns	—	—	0.01	—	**	87.10	96.77	1.43	2.55	
	mNRpP	**	**	**		-89.16		73.73	98.20	1.25	2.09	
	tNRpP	**	**	**	0.53	-98.87	**	41.60	99.68	10.92	—	
	TwANR	*	—	—	0.08	—	**	75.14	95.77	1.06	1.10	
	TwNR	**	**	**	0.55	—	**	27.00	98.67	10.96	—	
Root Anatomical Traits												
2013	mCRA (mm ²)	ns	**	ns	0.18	-9.57	**	56.96	0.81	0.89	1.38	
	mTSA (mm ²)	**	ns	ns	0.52	-0.28	**	51.03	0.12	1.45	3.78	
	mNXV	**	ns	*	0.14	+2.50	**	—	—	—	—	
	mRXSA (mm ²)	ns	**	ns	0.05	-8.22	**	52.18	0.83	0.81	0.95	
	mXVA (mm ²)	**	ns	ns	0.52	+0.97	**	76.43	—	1.51	2.53	
	mAXVA (mm ²)	*	*	ns	0.36	-2.99	**	60.69	—	1.42	2.40	
	tAXVA (mm ²)	ns	**	ns	0.40	-12.50	**	54.75	—	1.08	0.84	
	mXVA/mRXSA (%)	**	ns	**	0.10	-5.30	**	12.44	0.98	4.62	2.64	
	tXVA/tRXSA (%)	ns	*	ns	0.09	-14.87	**	68.16	0.98	1.89	4.80	
	tCRA (mm ²)	ns	ns	ns	0.22	+8.03	**	50.59	0.87	0.97	1.00	
	tTSA (mm ²)	ns	ns	ns	0.36	+6.56	**	53.17	0.15	1.88	5.65	
	tNXV	ns	ns	ns	0.35	+2.03	**	35.95	0.98	0.51	0.15	
	tRXSA (mm ²)	ns	ns	ns	0.21	+7.69	**	48.68	0.89	1.00	1.13	
	tXVA (mm ²)	ns	*	ns	0.24	-10.89	**	76.18	—	2.00	4.40	
	2014	mCRA (mm ²)	*	**	*	0.11	-14.63	**	39.56	0.94	1.10	1.70
mTSA (mm ²)		**	*	*	0.21	-4.12	**	38.41	0.95	0.76	0.82	
mNXV		**	**	ns	0.18	-4.89	**	28.13	0.94	0.50	0.64	
mRXSA (mm ²)		ns	**	ns	0.09	-16.94	**	38.64	0.94	0.86	1.24	
mXVA (mm ²)		**	**	ns	0.37	+8.63	**	63.17	0.98	2.25	8.89	
mAXVA (mm ²)		**	**	ns	0.26	+19.69	**	47.59	0.98	1.52	4.59	
tAXVA (mm ²)		**	**	ns	0.26	+11.50	**	56.26	0.98	2.34	8.10	
mXVA/mRXSA (%)		ns	**	ns	0.14	+64.71	**	70.24	0.99	2.90	10.1	
tXVA/tRXSA (%)		ns	ns	ns	0.12	-1.58	**	65.43	0.98	1.07	5.37	
tCRA (mm ²)		**	**	**	0.11	+11.93	**	42.18	0.97	0.92	1.11	
tTSA (mm ²)		**	ns	ns	0.35	+1.91	**	46.13	0.97	1.16	1.56	
tNXV		*	**	ns	0.29	-8.09	**	31.19	0.93	0.50	0.61	

(Continues)

TABLE 2 (Continued)

Year	Root Traits	Mean squares			H^2	E (%)	G	DTI CV	R (%)	Skew	Kur
		G	Dr	G*Dr							
	tRXSA (mm ²)	**	**	**	0.14	+10.84	**	41.76	0.97	0.95	1.11
	tXVA (mm ²)	**	ns	ns	0.30	+3.18	**	69.37	0.98	1.84	4.12

Abbreviations: * and **, significant effect at the 0.05 level (2-tailed) and 0.01 level (2-tailed), respectively; Dr, drought-treatment effect; DTI, trait drought tolerance indices; E, effect of drought stress on the anatomical traits; G CV, coefficients of genetic variation; G, genotypic effect; H^2 , broad sense heritability; Kur, kurtosis; mANR, arrested nodal roots of the main shoot axis; mAXVA, average area of the main shoot nodal root xylem vessel (mm²); mCRA, main shoot axis nodal root cortical area (mm²); mNRpP, number of nodal roots emerged at the main shoot axis; mNXV, Number of main shoot nodal root xylem vessels; mRGA, main shoot nodal root growth angle; mRXSA, main shoot nodal root cross sectional area (mm²); mTSA, main shoot nodal root stele area (mm²); mXVA, main shoot nodal root xylem vessel area (mm²); mXVA/mRXSA, main shoot nodal root xylem vessel area to cross sectional area ratio; ns, nonsignificant effect; R, repeatability; Skew, skewness; tANR, arrested nodal roots of the tiller; tAXVA, average area of the tiller nodal root Xylem vessel (mm²); tCRA, tiller nodal root cortical area (mm²); tNRpP, number of nodal roots emerged at the tiller; tNXV, number of tiller nodal root xylem vessels; tRGA, tiller nodal root growth angle; tRXSA, tiller nodal root cross sectional area (mm²); tTSA, main shoot nodal root stele area (mm²); TwANR, number of tiller with arrested nodal roots; TwANR, tillers with arrested number of nodal roots; TwNR, number of tiller per plant which formed nodal roots; TwNR, number of tillers with nodal roots; tXVA, tiller nodal root xylem vessel area (mm²); tXVA/tRXSA, tiller nodal root xylem vessel area to cross sectional area ratio.

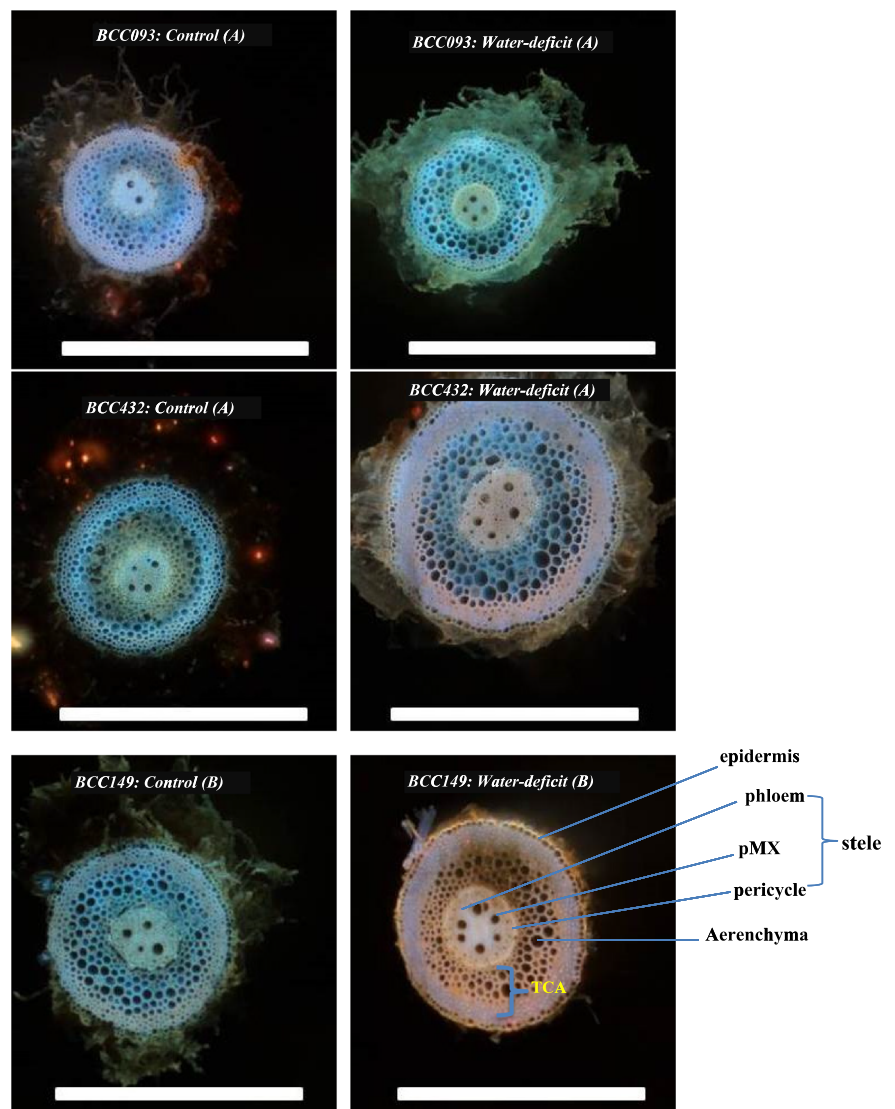


FIGURE 2 Cross-sectional views of the nodal root of the main axis/shoot (a) and tiller (b) showing genotypic differences in the root anatomical traits of three barley genotypes under unstressed and water-deficit stress conditions. The nodal roots of the main shoot (a) for genotypes BCC093 and BCC432 and of the tiller (b) for genotype BCC149 were ablated 1 cm from the base and analyzed. The images were obtained from laser ablation tomography. pMX, peripheral meta xylem vessels; TCA, total cortical area. The white scale bars on each root anatomical image = 1 mm

TABLE 3 Genotypic correlation coefficients among the architectural and anatomical drought tolerance trait indices of the studied panel

Traits	1	2	3	4	5	6	7	8	9	10	11	12	13	14	15	16	17	19	
1 mCRA	1																		
2 mTSA	0.65**	1																	
3 mRXSA	0.94**	0.67**	1																
4 mXVA	0.38**	0.82**	0.39**	1															
5 mAXVA	0.44**	0.81**	0.42**	0.90**	1														
6 tAXVA	0.08	0.21**	0.10	0.22**	0.28**	1													
7 mXVA/mRXSA	-0.12	0.18*	-0.22**	0.43**	0.37**	0.07	1												
8 tXVA/tRXSA	-0.03	0.16*	-0.04	0.29**	0.26**	0.39**	0.28**	1											
9 tCRA	0.22**	0.15*	0.25**	0.07	0.13	0.61**	-0.10	-0.07	1										
10 tTSA	0.07	0.24**	0.12	0.23**	0.26**	0.77**	0.06	0.22**	0.81**	1									
11 tNXV	0.07	-0.01	0.07	0.02	-0.03	-0.41**	0.09	0.22**	-0.22**	-0.39**	1								
12 tRXSA	0.22**	0.16*	0.25**	0.09	0.15*	0.61**	-0.07	-0.06	0.99**	0.81**	-0.15*	1							
13 tXVA	0.09	0.29**	0.12	0.38**	0.33**	0.89**	0.18*	0.49**	0.59**	0.81**	-0.30**	0.60**	1						
14 mRGA	-0.09	-0.08	-0.11	-0.01	-0.05	-0.09	0.04	-0.12	-0.08	-0.10	-0.07	-0.08	-0.04	1					
15 tRGA	-0.01	-0.09	-0.02	-0.05	-0.09	-0.04	-0.03	-0.05	-0.05	-0.08	0.05	-0.05	-0.04	0.22**	1				
16 mANR	0.23**	0.01	0.21**	-0.05	0.03	-0.02	-0.15*	0.01	0.12	-0.02	0.07	0.12	-0.08	-0.03	-0.02	1			
17 tANR	0.08	-0.06	0.07	-0.14	-0.08	0.13	-0.27**	-0.08	0.18*	0.11	-0.03	0.17*	0.07	-0.08	-0.02	0.30**	1		
19 TwANR	0.02	-0.08	0.02	-0.160*	-0.11	0.10	-0.29**	-0.07	0.12	0.09	-0.04	0.12	0.04	-0.03	0.01	0.26**	0.94**	1	

Abbreviations: mANR, arrested nodal roots of the main shoot axis; mAXVA, average area of the main shoot nodal root Xylem vessel (mm^2); mCRA, main shoot axis nodal root cortical area (mm^2); mRGA, main shoot nodal root growth angle; mRXSA, main shoot nodal root cross sectional area (mm^2); mTSA, main shoot nodal root stele area (mm^2); mXVA, main shoot nodal root xylem vessel area (mm^2); mXVA/mRXSA, main shoot nodal root xylem vessel area to cross sectional area ratio; tANR, arrested nodal roots of the tiller; tAXVA, average area of the tiller nodal root Xylem vessel (mm^2); tCRA, tiller nodal root cortical area (mm^2); tNXV, number of tiller nodal root xylem vessels; tRGA, tiller nodal root growth angle; tRXSA, tiller nodal root cross sectional area (mm^2); tTSA, tiller nodal root stele area (mm^2); TwANR, tillers with arrested number of nodal roots; tXVA, tiller nodal root xylem vessel area (mm^2); tXVA/tRXSA, tiller nodal root xylem vessel area to cross sectional area ratio. * and **, significant correlations between traits at 0.01 and 0.05 probability levels (2-tailed), respectively.

high ($R \geq 81\%$). Pearson correlation analysis performed based on genotypic mean showed varying degrees of correlations among the root traits (Table 3). High positive correlations ($r = .60-.99$; $P = .01$) were observed among root DTIs such as *mCRA* with *mTSA* and *mRXSA*; *mTSA* with *mRXSA*, *mXVA*, and *mAXVA*; *tAXVA* with *tXVA/tRXSA*, *tCRA*, *tTSA*, *tNXV*, *tRXSA*, and *tXVA*; *tTSA* with *tRXSA* and *tXVA*; *tCRA* with *tTSA*, *tRXSA* and *tXVA*. However, highest negative correlations were found for *tNXV* with *tAXVA* ($r = -.41$; $P = .01$), *tTSA* ($r = -.39$; $P = .01$), and *tXVA* ($r = -.30$; $P = .01$), followed by *mXVA/mRXSA* and *mRXSA* ($r = -.22$; $P = .01$). The number of main shoot arrested nodal roots (*mANR*) correlated low and positively with *mCRA* ($r = .23$; $P = .01$) and *mRXSA* ($r = .206$; $P = .01$); whereas, the main shoot xylem area to root area ratio correlated low and negatively with *tANR* ($r = -.269$; $P = .01$) and *TwANR* ($r = -.291$; $P = .01$).

3.2 | Population structure, linkage disequilibrium, and SNP marker statistics

Analysis of the population structure showed that the maximum ΔK occurred at $K = 2$, which means that the likely number of sub-populations in this panel is two (Figure 3a). With membership coefficient allotments of <0.6 , ~ 44 , and $\sim 48\%$ of the genotypes were inferred to belong to sub-population 1 and 2, respectively; whereas, 8% of the genotypes were considered hybrids (Figure S2). The PCoA plot (Figure 3b) revealed that the panel can be optimally delineated into two groups based on the barley row type (two- and six-row barley), with the first two principal coordinates contributing 21.93% of the genetic variations. We investigated whether there is phenotypic differences in the nodal root traits between the two-

and six-row barley (Figure 3c) and found out that the two groups did not differ significantly for the evaluated nodal root traits, except for *mXVA/mRXSA* in the 2013 planting.

Summary statistics of the genotypic data (Table S2) showed that the SNPs used for the GWAS analyses were evenly distributed across the 7 barley genome. They covered ~ 989.26 cM genetic distance. The SNP density across chromosomes ranged from 0.13 cM (in 5H) to 0.21 cM (in 1H), with the largest gap ranging from ~ 4.46 cM on 2H to ~ 10.27 cM on 4H. Since chromosomal LD decay of this panel extends between 2.03 cM (4H) and 4.91 cM (7H) (Table S2; Figure S3), we concluded that the number of SNPs required for adequate genome coverage and detection of causal QTL was met.

3.3 | QTL associated with nodal root response to water-deficit stress in barley

GWAS was performed using 22 root traits and 8987 SNPs. A total of 83 SNPs comprising of 58 and 25 SNPs for anatomical and morphological traits, respectively, were associated with the root response to water deprivation in the diversity panel (Table S3; Figure S4). They were detected across all the barley chromosomes with the exception of 2H and explained between 0.5 and 5.9% of the observed variation. The highest number of MTAs was detected on chromosomes 3H (22) and 5H (22), while 10 of the detected SNPs were not assigned to the barley genetic map, although we obtained their physical positions (bp) *via in silico* in the IPK database (http://webblast.ipk-gatersleben.de/barley_ibsc/). The analyses of the genomic regions of the significant SNPs indicated that most of them cosegregate with genes whose gene ontology (GO) terms are related to

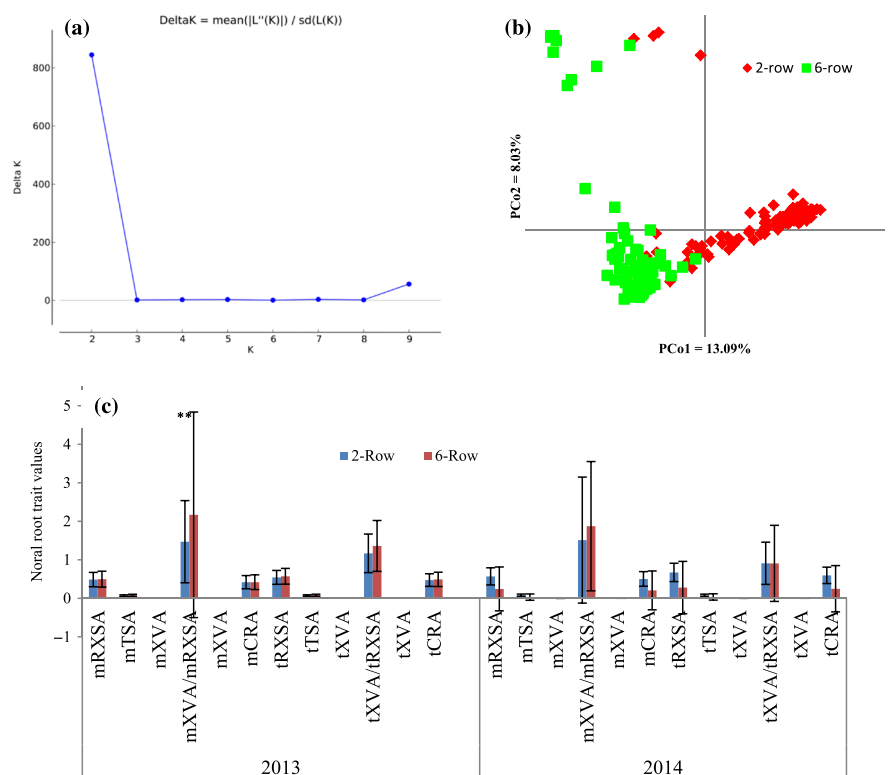


FIGURE 3 (a) Population structure analysis inferred using the using the Evanno ΔK method (Evanno et al., 2005) and based on 20 independent runs and K ranging from 2 to 9. The maximal ΔK occurred at $K = 2$; (b) principal coordinate analysis based on 8,987 SNP/GTBS markers showing a scatter plot of PCo1 (explaining 13.09% of the variance) versus PCo2 (explaining 8.03% of the variance). Colors are according to the barley row-type (two-row, red; six-row, green); and (c) phenotypic variations in root anatomical trait response to drought between two-row and six-row barley. The error bars are presented for each barley row-type

root development and stress responses in several plant species (Table S4). Using the chromosomal LD of the panel (2.03 cM in 4H–4.91 in cM in 7H), the 83 significant SNPs were assigned into 11 genetically linked QTL intervals (Figure 4). Four QTL intervals, including *QTL-3H_1*, *QTL-3H_2*, *QTL-3H_3*, and *QTL-3H_4*, were found on 3H. The *QTL-3H_1* spanning an interval of ~0.66 cM was detected for *tXVA* and *mNXV* in 2013 and 2014, respectively; while *QTL-3H_2* located between 49.7 and 52.0 cM associated with *tXVA* and root growth angle (in 2013, 2014, and 2015). The “*QTL-3H_4*” at ~146 cM exhibited a pleiotropic effect on number of nodal roots (TNRp) and stagnated nodal roots (tANR) in 2014 and 2015, respectively. In addition, the *QTL-5H_1* spanning from ~23.3 to 26.8 cM on 5H had a considerable effect on anatomical (*mTSA* and *tXVA*) and architectural (*TwANR*) nodal root traits; while locus at 109.7 cM—“*QTL-5H_3*” on 5H strongly influenced nodal root variations observed in *tCRA* and *tRXSA* in

2013. Most of these intervals were found to be in proximity to QTL previously reported for drought tolerance in wheat (Table 4). Analysis of SNP effect on *QTL-5H_3* locus showed that genotypes carrying the “C” allele had higher root drought tolerance values than those with “T” alleles in 2013 and 2014 (Figure 5).

3.4 | Identification of epistatic interactions for nodal-root response to water-deficit stress

Genome-wide SNP–SNP interaction analysis was performed to gain additional insights into the genetic architecture of nodal root response to water-deficit stress that may explain new heritable genetic components. A total of 44 epistatic QTL involved in

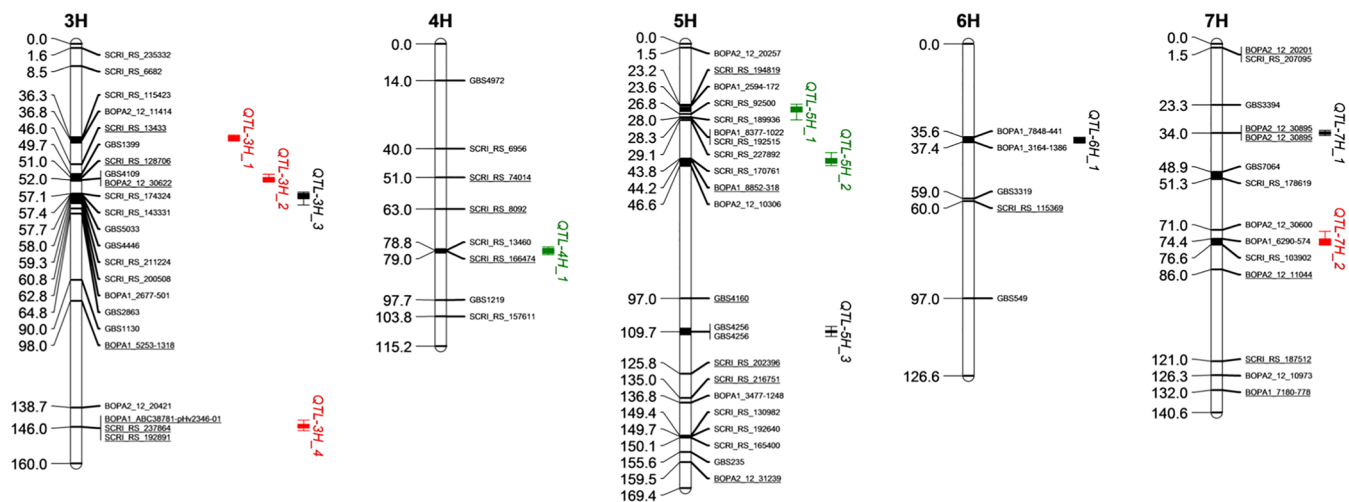


FIGURE 4 Chromosomal location of the associated SNPs for all investigated root architectural and anatomical traits as revealed by GWAS analyses. The vertical black lines in chromosomes denote the maker interval in LD where SNPs were located. The QTL name is shown on the right: QTL for DTIs in both planting seasons (in red), DTIs for both root architectural and anatomical (in green), and nodal root DTIs for either architectural or anatomical (in black) traits are shown in the figure. The underlined markers are associated with the morphological root traits

TABLE 4 QTL intervals associated with water-deficit response and adaptation in the 192 diversity barley panel

QTL Interval	Chr	Associated Root Traits	Reported QTL/Gene in the Region
QTL3H_1	3H	<i>tXVA</i> and <i>mNXV</i>	Nodal root system size, plant height, harvest index and grain yield (Chloupek et al., 2006)
QTL-3H_2	3H	<i>tRGA</i> (in 2013, 2014, and 2015) and <i>mAXVA</i>	Plant height and a semi-dwarf single recessive gene <i>uzu gene</i> (Chono et al., 2003; Pasam et al., 2012)
QTL-3H_3	3H	<i>tXVA</i> and <i>mCRA</i>	Heading date that was found in the domain of circadian clock/photoperiod pathway homologous gene (Pasam et al., 2012)
QTL-5H_2	5H	<i>tXVA</i> and <i>tAXVA</i>	Relative-water content and osmotic adjustment (Teulat et al., 2001)
QTL-5H_3	5H	<i>tCRA</i> and <i>tRXSA</i>	Heat-stress, stay green (Gous et al., 2016), and root length/root-shoot ratio (Arifuzzaman et al., 2014), DTI for water content (Gudys et al., 2018); water use efficiency and net photosynthetic rate (Wójcik-Jagła et al. 2013; 2018)
QTL-7H	7H	<i>tNRpP</i>	Harvest index, day to heading yield, water absorption, and plant height (Pillen, Zacharias, & Leon, 2003)

Abbreviations: *mAXVA*, average area of the main shoot nodal root xylem vessel (mm^2); *mCRA*, main shoot axis nodal root cortical area (mm^2); *mNXV*, number of main shoot nodal root xylem vessels; *tAXVA*, average tiller nodal root xylem vessel area (mm^2); *tCRA*, tiller nodal root cortical area (mm^2); *tNRpP*, number of nodal roots emerged at the tiller; *tRGA*, tiller nodal root growth angle; *tRXSA*, tiller nodal root cross sectional area (mm^2); *tXVA*, tiller nodal root xylem vessel area (mm^2).

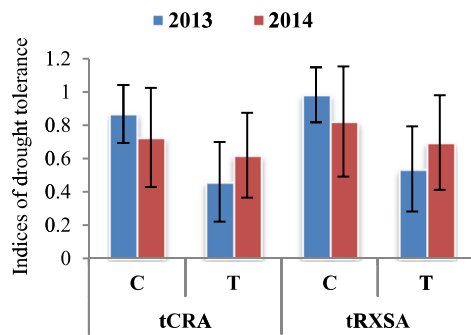


FIGURE 5 Bar chart showing allele effects of SNP GBS4256 (P -values $\leq 8.10E-06$) on tCRA (tiller nodal root cortical area) and tRXSA (tiller nodal root cross sectional area) drought tolerance indices in 2013 and 2014 planting seasons

25 epistatic interactions were identified (Table 5; Figure 6). They explained between 19.98 and 41.60% of the observed variations. Among them are 13 loci on 3H, 4H, 5H, and 7H that were also detected via GWAS to exert additive main effects on the nodal root variations under water-deficit stress. The largest number of epistatic QTL were found on 5H (14) and 6H (9), including a locus at ~ 50 cM, which is in LD with another main effect QTL, that interacted epistatically with eight additional loci. BLAST searches indicates that most of significant epistatic loci are situated in the vicinity of genes involved in root-water stress response. Analysis of the effect of the interacting SNP pairs [at 118.48 cM (1H – SCRI_RS_147611; T/C) and 96.73 cM (5H – SCRI_RS_175290; C/T)] on the nodal root traits indicated that genotypes having allele combination “C*T” performed $\sim 32.58\%$ higher than those with alleles “T*C”; whereas the combination of “A*C” alleles of locus at 118.48 cM (1H – SCRI_RS_147611; T/C) and locus at 111.32 cM (5H – SCRI_RS_136812; G/A) increased the nodal root DTI values by 29.37% relative to the “G*T allele combination (Figure 7). In addition, locus at 132.58 cM (for BOPA1_3179-497; A/G) on 2H interacted epistatically with another locus at 69.11 cM (for GBS3992; G/A) on 7H, and their allele combination of “A*A” increased the root DTI values by 40.66% higher than the G*A allele.

3.5 | Identification of candidate genes associated with QTL for nodal root responses to water deficit

To explore candidate genes at the vicinity of the detected QTL, searches were made with the core sequences of the significant SNPs. BLAST results indicated that some of the SNPs are collocated or cosegregated with genes whose biological functions are related to root response to water-deficit stress (Table S4). For instance, the SNP locus at 52.03 cM on 3H (QTL-3H_2) for tRGA and mAXVA is physically linked to ZIFL2 (HORVU3Hr1G043300) that regulates *basipetal auxin transport*, *root gravitropism*, *root*

development, *regulation of stomatal closure*, and *response to water deprivation*. SNP locus at 109.65 for tCRA and tRXSA on 5H (QTL-5H_3) corresponds to the domain of MATE efflux family protein (MATE, HORVU5Hr1G086830.4); while the locus at 86 cM (BOPA2_12_11044) on 7H (QTL-7H) for tNRpP (number of tiller nodal roots) cosegregated with *Peptidyl-prolyl cis-trans isomerase* (PPIB, HORVU7Hr1G095720) that is catalyzed by LATERAL ROOT-LESS2 (LRT2). Despite the strong candidacy and collocation of these SNPs with genes involved in root development and response to water deprivation, we identified other possible candidate genes in the vicinity (≤ 5 Mb up and downstream) of the significant QTL (Table S5). The QTL-3H_2 is located between 275846137 and 283488520 bp (~ 7.64 Mbp) on 3H and contains 20 HC genes, Out of which one additional candidate genes were identified. The QTL-5H_3 interval (~ 8.35 Mbp) on 5H revealed a total of 123 HC genes. Among them are six genes that induce variational changes in root traits during water stress. A total of 66 HC genes were identified in the QTL-7H interval (~ 9.27 Mbp); out of which functions of nine genes could be potentially linked to root water-deficit stress-related responses.

Genome-wide two-locus epistatic interactions uncovered a total of 44 epistatic interacting loci that are physically located in the domain of some important root responsive genes (Table 5). The locus at 118.48 cM (1H) in the *auxin response factor 15* (ARF15) domain epistatically interacted with two loci at 96.73 and 113.32 cM on 5H corresponding to the protein domains of Protein kinase superfamily (PBS) and SAUR-like auxin-responsive family (SAUR), respectively. In addition, SNP loci corresponding to *RNA-binding protein 1* (RBG1) interacted epistatically with locus at 69.11 cM (GBS3992; G/A) on 7H. An additive main effect QTL identified by GWAS in the major facilitator superfamily protein domain on 5H also had epistatically interaction with eight loci on 2H, 4H, 5H, 6H, and 7H corresponding to important gene domains, including *Receptor-like protein kinase* (at 152.36 cM on 5H), a key regulator of root hair development.

4 | DISCUSSION

A comprehensive understanding of how roots adapt to stress due to water deficit remains a valuable goal as roots act as sensors for detecting changes of soil water status. Barley roots are composed of axes arising first from: (a) *primordia* in the seed (seminal/primary roots) and (b) nodes (nodal/crown roots) of the main shoot and tillers. Both primary and nodal root responded differently to soil water deprivation, and the number and length of nodal roots are governed by environmental factors (Kuhlmann and Barraclough, 1987; Rostamza et al., 2013). In this study, the variability in nodal root architecture and anatomy were exploited to elucidate the genetic basis of nodal root response to water-deficit stress in a barley diversity panel. There was wide genotypic variation in the evaluated root phenotypes in response to water-deficit stress, with moderate H^2 and high R for the root traits. This suggests that the

TABLE 5 List of epistatic interaction SNP pairs and their corresponding genes identified for nodal root responses to water deficit in the GWAS panel

Marker	Chr1	pos1	Annotation	Marker	Chr2	pos2	Annotation	F_Val	Prob	Epi_FDR	
	SNP1										
GBS2168	1H	47.83		GBS3506	4H	78.68		19.24	1.54E-10	8.22E-07	
SCRI_RS_147611	1H	118.48	Auxin response factor 15	SCRI_RS_149094	1H	130.74	F-box family protein	27.90	7.25E-15	1.49E-11	
SCRI_RS_147611	1H	118.48	Auxin response factor 15	SCRI_RS_175290	5H	96.73	Protein kinase superfamily protein	31.67	1.72E-16	1.94E-12	
SCRI_RS_149094	1H	130.74	F-box family protein	BOPA1_2765-406	3H	32.68		18.85	1.12E-10	3.98E-09	
GBS6105	2H	86.61		SCRI_RS_175290	5H	96.73	Protein kinase superfamily protein	26.60	4.67E-14	3.95E-11	
GBS2883	3H	15.16	Core-2/1-branching beta-1,6-N-acetylglucosaminyltransferase protein	SCRI_RS_136812	5H	111.32	SAUR-like auxin-responsive protein family	24.23	5.95E-13	1.74E-10	
GBS2283	3H	57.37	Anoctamin-like protein	SCRI_RS_136812	5H	111.32	SAUR-like auxin-responsive protein family	21.42	9.07E-12	8.63E-10	
GBS2283	3H	57.37	Anoctamin-like protein	SCRI_RS_143790	1H	132.37	Pentatricopeptide repeat-containing protein	22.57	2.70E-12	4.32E-10	
BOPA2_12_30325	3H	77.12		GBS93	6H	82.37		13.78	5.38E-07	8.72E-05	
GBS3595	4H	4.16		GBS6804	2H	106.86		15.47	2.37E-08	2.42E-06	
GBS6902	4H	44.00	Homeobox protein knotted-1-like 4	SCRI_RS_136812	5H	111.32	SAUR-like auxin-responsive protein family	22.38	3.22E-12	4.74E-10	
GBS6902	4H	44.00	Homeobox protein knotted-1-like 4	SCRI_RS_149094	1H	130.74		24.92	2.32E-13	1.02E-10	
BOPA2_12_30824	4H	52.34		GBS1694	1H	12.46		14.79	1.88E-07	6.05E-05	
BOPA1_6464-1115	4H	63.24	GDP-mannose transporter GONST3	SCRI_RS_149094	1H	130.74	F-box family protein	20.61	1.62E-11	1.17E-09	
GBS3506	4H	78.68	Kelch-like protein 25	GBS3992	7H	69.11	Glutamate receptor 2.7	25.99	1.95E-10	8.22E-07	
GBS3506	4H	78.68	Kelch-like protein 25	GBS5648	4H	111.97		17.59	8.43E-10	1.03E-06	
GBS3506	4H	78.68	Kelch-like protein 25	SCRI_RS_156871	2H	67.92	Gamma-tubulin complex component 2	19.02	1.55E-10	8.22E-07	
GBS2128	5H	44.10		GBS2165	6H	50.21		19.85	8.65E-10	4.81E-09	
GBS2128	5H	44.10		SCRI_RS_169829	6H	50.21	Protein vernalization insensitive 3	22.56	1.61E-11	3.56E-10	
GBS1065	5H	50.00	Major facilitator superfamily protein	GBS21	5H	68.3		13.06	8.16E-07	9.70E-05	
GBS1065	5H	50.00	Major facilitator superfamily protein	GBS4202	7H	47.73		15.54	5.74E-08	5.72E-05	
GBS1065	5H	50.00	Major facilitator superfamily protein	GBS5159	2H	74.08		15.86	3.57E-08	4.85E-05	
GBS1065	5H	50.00	Major facilitator superfamily protein	GBS5774	5H	130.35		13.92	8.24E-07	9.70E-05	
GBS1065	5H	50.00	Major facilitator superfamily protein	GBS6529	5H	23.61	Cationic amino acid transporter 2	13.98	1.99E-07	6.26E-05	
GBS1065	5H	50.00	Major facilitator superfamily protein	GBS93	6H	82.37		12.54	7.87E-07	9.70E-05	

(Continues)

TABLE 5 (Continued)

Marker	Chr1	pos1	Annotation	Marker	Chr2	pos2	Annotation	F_Val	Prob	Epi_FDR
GBS1065	5H	50.00	Major facilitator superfamily protein	SCRI_RS_102066	5H	152.36	Receptor-like protein kinase	12.84	5.13E-07	8.72E-05
GBS1065	5H	50.00	Major facilitator superfamily protein	SCRI_RS_235738	4H	57.51	Filament-like plant protein 4	16.10	1.27E-07	6.04E-05
BOPA1_1786-297	5H	65.39	1-aminocyclopropane-1-carboxylate oxidase 1	GBS2165	6H	50.21		22.40	2.44E-11	4.48E-10
GBS6962	5H	98.13		SCRI_RS_236114	5H	152.47	Trafficking protein particle complex subunit 4	14.00	8.97E-07	1.38E-05
GBS2497	5H	99.93		GBS6514	2H	62.75		23.68	1.07E-12	1.42E-11
GBS1572	5H	109.65		GBS2165	6H	50.21		31.54	2.64E-11	4.71E-10
SCRI_RS_136812	5H	111.32	SAUR-like auxin-responsive protein family	SCRI_RS_143790	1H	132.37	Pentatricopeptide repeat-containing protein	22.12	3.05E-12	4.55E-10
SCRI_RS_136812	5H	111.32	SAUR-like auxin-responsive protein family	SCRI_RS_147611	1H	118.48	Auxin response factor 15	25.40	9.48E-14	5.94E-11
BOPA2_12_31123	5H	169.38	Plant invertase/pectin methylesterase inhibitor superfamily protein	GBS3992	7H	69.11		17.97	4.37E-10	8.22E-07
GBS369	6H	3.75		SCRI_RS_136812	5H	111.32	SAUR-like auxin-responsive protein family	22.65	2.48E-12	4.12E-10
GBS2165	6H	50.21		SCRI_RS_206061	5H	84.51	NAC domain containing protein 41	21.20	1.01E-10	1.11E-09
GBS4346	6H	55.45		GBS5094	5H	169.38		15.81	6.67E-08	5.72E-05
GBS5031	6H	77.54		GBS920	4H	102.12		36.76	5.30E-18	1.25E-15
GBS6333	6H	92.23		GBS7226	2H	114.24		18.43	5.35E-06	1.63E-05
BOPA1_8200-978	7H	1.49	Kelch repeat-containing protein	BOPA2_12_30993	4H	48.65	O-methyltransferase family protein	35.04	1.70E-16	1.61E-12
GBS1183	7H	13.88		GBS6333	6H	92.23		16.42	4.59E-06	1.53E-05
GBS3992	7H	69.11		BOPA1_3179-497	2H	132.58	RNA-binding protein 1	18.56	2.30E-10	8.22E-07
GBS3992	7H	69.11		GBS5288	3H	83.63		18.42	3.09E-10	8.22E-07
BOPA2_12_10652	7H	102.34		GBS3207	7H	73.16		20.18	3.14E-07	7.09E-05

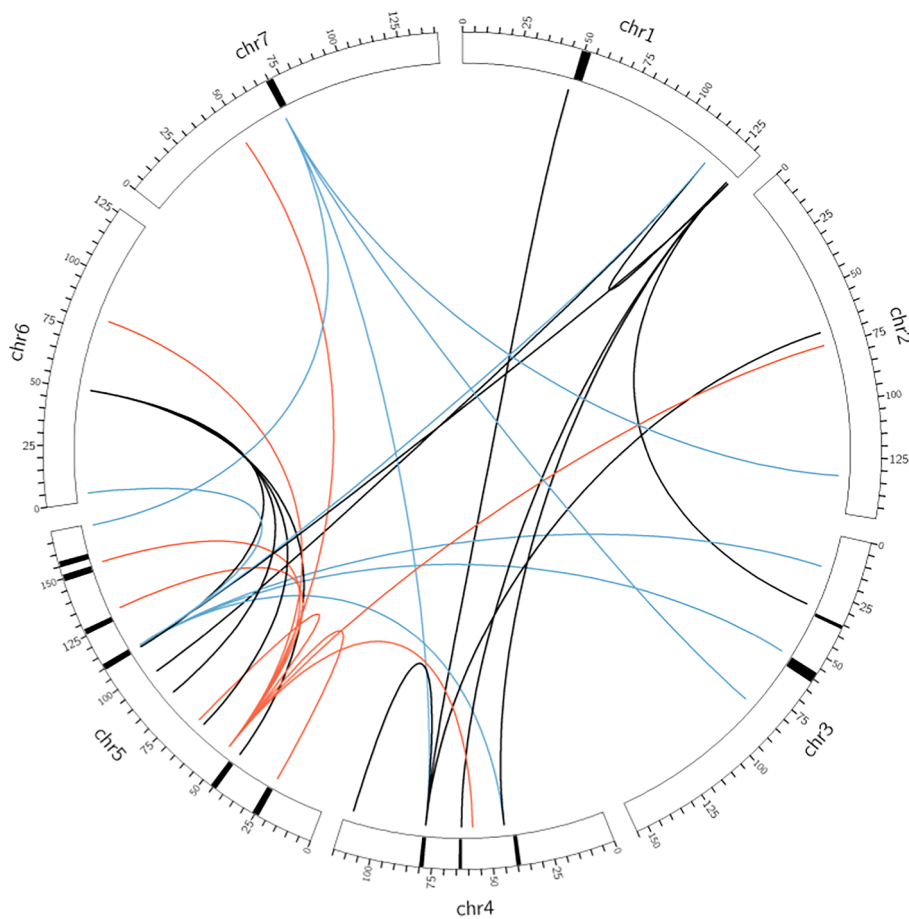


FIGURE 6 Circular plot showing the epistatic interactions with the corresponding locations on the genetic map of barley. Barley chromosomes 1H–7H are shown in a clockwise direction in the Circos diagram. Colored connections represent epistatic loci controlling different root anatomical DTI traits. QTL intervals showing main effects on the root response to drought are in black

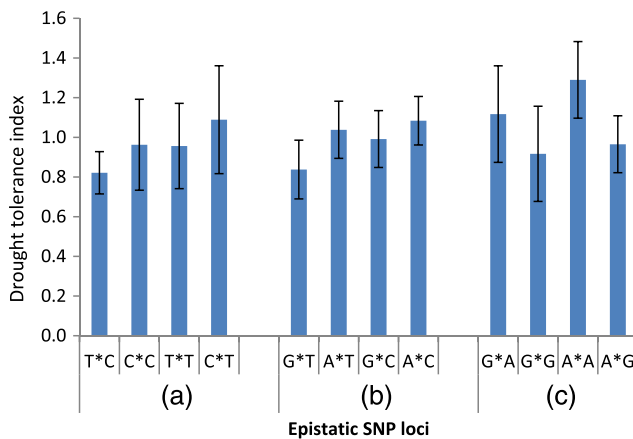


FIGURE 7 Effects of allele combinations including (a) 118.5 cM (1H)*96.7 cM (5H), (b) 118.5 cM (1H)*111.3 cM (5H), and (c) 132.6 cM (2H)*69.1 cM (7H) involved in the epistatic interactions observed in the nodal root responses to water-deficit stress

evaluated root phenotypes can be exploited to gain genetic and molecular insights into the responses of barley roots to prolonged soil water depletion, to support long-term breeding efforts toward developing drought-tolerant barley cultivars.

4.1 | Effects of water-deficit stress on root architecture

Water-deficit stress induced larger root growth angles of the main shoot (*mRGA*) and tillers (*tRGA*) in 2013 and 2015. Increase in root growth angles enhances the ability of plants to avoid drought stress (Uga et al., 2013). Subsequently, this may translate to steeper and deeper root systems that allow plants to access water in deeper soil strata. The number of arrested nodal roots increased, while the number of nodal root per plant decreased during water-deficit stress, an indication that the soil water depletion suppresses nodal root post-emergence, root growth (Sebastian et al., 2016), and decreases the number of nodal/lateral roots (Zhan et al., 2015; Gao and Lynch, 2016). The reduction in the number of nodal root during water-deficit stress scenarios may be connected to the plant's adaptive response to improve the drought stress tolerance by reducing the metabolic costs of soil exploration, permitting greater axial root elongation, greater rooting depth, and hence greater water acquisition from drying soil (Lynch et al., 2014; Saengwilai et al., 2014; Zhan et al., 2015). Reports have shown that increased number of arrested roots (which is a direct consequence of reduced supply of carbohydrate) in plants under water-deficit stress would reduce metabolic energy costs and conserve water (Fujita et al., 2006; Szalai et al., 2010; De Smet et al., 2003; Ristova et al., 2017).

4.2 | Effects of water-deficit stress on root anatomy

Nodal root cortical area, root stele area, and total root area decreased under water-deficit stress in main shoot nodal roots, but increased in the tiller nodal roots. The observed contrasting response may be connected to the different adaptive role the main shoot and tiller nodal roots plays during drought. Reduction in the main-shoot nodal roots may be presumably attributed to root growth allometry and/or the vital role the main shoot nodal roots plays during soil water limitation. This might be due to the fact that the main shoot borne nodal roots explores the deeper subsoil that could contain more water as opposed to the tiller nodal roots. Lynch (1995) and Strock et al. (2018) have reported that smaller root cross-sectional area induced by plants adaptive response of decreased root secondary growth increases root length (for greater soil exploration) and improves the consumption of growth-limiting resources. Growth allometry is induced by multiple cryptic genetic factors associated with local climate and abiotic stress response (Vasseur et al., 2018), suggesting that the contrasting response of tiller and main-shoot nodal roots may be an adaptive response to water deficit. Thus, may warrants further investigation as a potential root breeding target. Even more so as the presence of smaller diameter roots under soil water scarcity is considered a strategy to maximize absorptive surfaces and increase rates of water and nutrient uptake (Eissenstat, 1992).

Richards and Passioura (1989) indicated that root metaxylem vessel regulates crop WUE if water is available in the subsoil, but the top soil is dry. Our findings indicate that water-deficit stress increased the number of xylem vessels, which is in line with reports in rice and wheat (Kadam et al., 2015) and maguey (Peña-Valdivia & Sánchez-Urdaneta, 2009). Increase in the number and thickness of xylem vessels improve tolerance to cavitation, thus would confer resistance to drought (Arend and Fromm, 2007; Awad et al., 2010). The formation of thick-walled and suberized cell layers at the periphery of the root and around the stele was evident in the water stressed roots. This is an adaptive response to water deficit (Lo Gullo et al., 1998), to enable plants regulate the flux of water from the root to the soil (Hose et al., 2001) and prevent the desiccation of meristematic tissues that is, pericycle and other tissues inside the stele (North and Nobel, 1992). The suberization and lignification of roots affect radial water conductance and may help reduce water loss from mature roots into the dry soil (Lynch et al., 2014). Root cortical cell size (CCS) and root cortical aerenchyma (RCA) increased under water-deficit stress, as has been observed in maize by Chimungu et al. (2014) and Zhu et al. (2010), respectively. Larger CCS and RCA are beneficial to plants under water stress because it reduces respiration, nutrient content of root tissues, and the metabolic cost of soil exploration (Zhu et al., 2010; Postma and Lynch, 2011; Chimungu et al., 2014; Lynch et al., 2014; Saengwilai et al., 2014; York et al., 2015) to support increased rooting depth by reducing the proportion of cortical tissue occupied by cytoplasm and by transforming living cortical cells into air space.

4.3 | Population structure and relationships

The bayesian clustering algorithm identified two ($K = 2$) subpopulations in the studied panel, which is in concordance with the PCoA result. The clustering pattern of the panel was based on two- and six-row barley type. The LD analyses revealed that the panel extends over short distances from 2.03 (in 4H) to 4.91 cM (in 7H) when compared to the LD decay of over 10 cM reported in barley (Hamblin et al., 2010; Mezaka et al., 2013; Bellucci et al., 2017), an indication that the panel is genetically diverse due to several recombination events that may have occurred throughout their evolutionary history. With the observed SNP density of between 0.13 (5H) and 0.21 cM (1H) in the panel, it is expected that sufficient marker coverage for high resolution and detection of casual QTL was achieved.

4.4 | Identification of QTL associated with root responses under water deprivation stress

GWAS identified a total of 83 SNPs, distributed in 11 QTL intervals to be associated with the nodal root architectural and anatomical response to water-deficit stress. Most of the identified SNPs exhibited pleiotropic effects on the root traits across seasons and are proximal to QTL reported for osmotic potential, root elongation, water-soluble carbohydrate, accumulation of water-soluble carbohydrate, stay green, heat stress, and drought responsive root/yield-related traits (Diab et al., 2004; Raman et al., 2005; von Korff et al., 2008; Pasam et al., 2012; Arifuzzaman et al., 2014; Gous et al., 2016). The mechanisms and traits related to WUE, deeper root growth, photosynthesis, and mobilization of photosynthates to grain production are tightly linked to crop adaptive responses to drought stress (Zama-Allah et al., 2011; Marajo et al., 2015; Polanyi Promo et al., 2017).

Because the SNPs identified by GWAS may in some cases unlikely represent true causal genetic variants, but rather one in high LD with the gene or regulatory element affecting the observed variation, we considered the genomic intervals in high LD with the significant SNPs as one gene locus (QTL interval). The *QTL3H_1*, controlling water-deficit responses for xylem area-related traits, is proximal to QTL for nodal root system size, plant height, harvest index, and grain yield (Chloupek et al., 2006). *In silico* analysis of the associated *QTL-3H_2* interval revealed that it overlaps with *SNP313* harboring QTL for plant height and a semi-dwarf single recessive gene *uzu* (Chono et al., 2003; Pasam et al., 2012) reported to correlate highly with relative water content and stress tolerance (drought and salinity) in barley DH lines. The *QTL-3H_3* interval coincides with *SNP340* (59.89 cM) locus for heading date located in the domain of circadian clock (Pasam et al., 2012), suggesting that *QTL-3H_3* may be linked to drought avoidance traits. The expression of circadian clock genes is induced by osmotic stress in the barley root systems (Habte et al., 2014). The *QTL-5H_2* associated with *tXVA* and *tAXVA* was found in the vicinity of *Q5HA* reported

for relative water content and osmotic adjustment (Teulat et al., 2001). *In silico analysis of the QTL-5H_3* showed that it cosegregates with a diagnostic DArT-marker (*bPb-5529*) detected for heat stress, stay green (Gous et al., 2016), and root length/root-shoot ratio (Arifuzzaman et al., 2014) and proximal to QTL detected for water content, WUE, and net photosynthetic rate (Gudys et al., 2018; Wójcik-Jaęła et al., 2013; 2018). The coincidence of the significant QTLs detected in this study with those previously reported for drought stress adaptive response strongly suggest that they may be linked to genes involved water-deficit response, thus can be exploited to unravel the genetic control and molecular players responsible for root variable responses to soil water depletion.

4.5 | Candidate genes in the detected QTL regions for root water-deficit response

Because major responses of plants to water-deficit stress occur at the molecular level *via* the induction of water stress-responsive genes (Chen & Xiong, 2012), BLAST search was performed in the IPK barley database to identify the genes cosegregating with the significant SNPs detected in this study. The pleiotropic locus at 52.03 cM on *QTL-3H_2* associated with root angle and main shoot nodal root Xylem vessel is physically located in the *ZIFL2* (HORVU3Hr1G043300) domain. In *Arabidopsis*, ZIFL superfamilies play key roles in auxin transport, root gravitropism, regulation of stomatal closure, response to karrikin/water deprivation, and root growth and development (Nelson et al., 2010; Remy et al., 2013). Genes controlling traits related to stomatal development and guard cell movements strongly impact the WUE in plants (Ruggiero et al. (2017) and may serve as a potential target for molecular breeding programs. Another pleiotropic SNP at 109.65 cM on 3H is cosegregating with *MATE efflux family* (*MATE*; HORVU5Hr1G086830). *MATE* modulates abscisic acid efflux and ABA sensitivity responses to drought stress (Takanashi et al., 2014; Jarzyniak and Jasinski, 2014; Zhang et al., 2014). SNP (*BOPA2_12_11044*) at 86 cM on 7H associated with the observed variations in the number of nodal roots is physically located in the domain of *PPIB* (HORVU7Hr1G095720). *PPIB* is catalyzed by *LATERAL ROOTLESS2* to regulate root gravitropism, lateral root development, and induce thermo-tolerance (Xi et al., 2016; Kaur et al., 2016). Root gravitropism is a physiological drought response that redirects root growth by gravitational pull toward the down water sources *via* auxin transport. The mechanisms of auxin transport have also been implicated in this process (Blancaflor, 2013; Sato et al., 2014; Shin et al., 2005). The associated QTL intervals: *QTL-3H_2*, *QTL-5H_3*, and *QTL-7H* were further scanned for detection of other possible candidate genes by searching 1–5 Mbp up- and down-stream away from the genes cosegregating with the significant SNPs (de Koning and Haley, 2005; Ge et al., 2009). We identified two (*QTL-3H_2*), seven (*QTL-5H_3*), and six (*QTL-7H*) additional candidate genes whose molecular functions determine the outcome of root adaptive responses to root water stress response in these regions.

4.6 | Epistatic interactions are involved in root trait responses to water deprivation

Epistasis may play an essential role in trait improvement and improves the selection efficiency (Jannink & Wu 2003; Jannink, Moreau, Charmet & Charcosset, 2009). In this study, 13 out of the 44 identified epistatic QTLs also had additive main effect on the nodal root anatomical response to water-deficit stress, an indication that the nonadditive contributions of these loci should not be neglected in the barley root breeding program. Some of the interacting loci detected are cosegregating with genes for drought stress responses. The locus at 118.48 cM on 1H cosegregate with *ARF15* and interacted epistatically with 113.32 cM (1H) and 96.73 cM (5H) SNP loci whose sequences are domiciled in the *SAUR* and *PBS* gene domains, respectively. *ARF15* has been implicated in the activation and repression of early/primary auxin response genes such as *Aux/IAA* and *SAUR* gene families (Hagen and Guilfoyle, 2002; Ulmasov et al., 1997, 1999), especially during water-deficit stress. Reports have also shown that the overexpression of *SAUR* under salt and drought results in higher root length, survival rate, and improved drought/salt tolerance in *Arabidopsis* plants (Guo et al., 2018). The *PBS* gene families positively regulate drought stress in plants *via* ABA pathways, stomatal responses, and root growth (Wang et al., 2016; Cui et al., 2018). Two loci at 132.58 cM on 2H coding for *RBG1* and at 69.11 cM on 7H interacted epistatically with each other. Reports have shown that *RBG1* regulates tolerance to salt and drought stress (Ambrosone et al., 2015) and root growth (Shida et al., 2015). The main-effect QTL at 50.0 cM is in the vicinity of major facilitator superfamily (MFS) protein on 5H. Our result indicated that it is epistatically interacting with eight loci on 2H, 4H, 5H, 6H, and 7H that code for several genes, including locus at 152.36 cM domiciled by *Receptor-like protein kinase* (RLK) on 5H. MFS plays a vital role in polar auxin transport and drought stress tolerance (Remy et al., 2013), while Wei and Li (2018) have implicated RLK in the regulation and controlling of root hair development.

In conclusion, this study identified important chromosomal regions harboring candidate genes that might be involved in the architectural and anatomical nodal root response to water-deficit stress in Barley. Going forward, the QTL and genetic variants identified are potential resources for root-targeted breeding for important traits, like drought tolerance improvement in barley.

ACKNOWLEDGEMENTS

The work was mainly supported by the DFG Grant PAK 770 and was partly funded institutionally by IBG-2 (Plant Sciences), Forschungszentrum Jülich/Helmholtz Association, Germany. The GBS data analyses were provided by Jeannette Lex and Tina Lüders from JKI, Quedlinburg, Germany.

CONFLICT OF INTEREST

The authors declare that the study was conducted in the absence of any commercial or financial relationships that could be envisaged and/or construed as a conflict of interest.

AUTHOR CONTRIBUTION

AB and JL conceived and acquired the project research grant; AB, JL, JP, JPL, and TW planned the experiments; JP and TW collected the data; AB, AAN, BCO, JL, JP, JPL, and TW analyzed/interpreted and prepared the manuscript; and all authors approved the manuscript.

ORCID

Benedict C. Oyiga  <https://orcid.org/0000-0001-5547-2572>

Jonathan P. Lynch  <https://orcid.org/0000-0002-7265-9790>

REFERENCES

- Ahanger, M. A., Tyagi, S. R., Wani, M. R., & Ahmad, P. (2014). Drought tolerance: Role of organic osmolytes, growth regulators, and mineral nutrients. In *Physiological mechanisms and adaptation strategies in plants under changing environment* (pp. 25–55). New York, NY: Springer.
- Ambrosone, A., Batelli, G., Nurcato, R., Aurilia, V., Punzo, P., Bangarusamy, D. K., et al. (2015). The Arabidopsis AtRGGGA RNA binding protein regulates tolerance to salt and drought stress. *Plant Physiology*, *168*, 292–306.
- Arai-Sanoh, Y., Takai, T., Yoshinaga, S., Nakano, H., Kojima, M., Sakakibara, H., et al. (2014). Deep rooting conferred by DEEPER ROOTING 1 enhances rice yield in paddy fields. *Scientific Reports*, *4*, 5563.
- Marajo, S. S., Beebe, S., Crespi, M., Delbreil, B., Gonzalez, E. M., Gruber, V., et al. (2015). Abiotic stress responses in legumes: Strategies used to cope with environmental challenges. *CRC Critical Reviews in Plant Sciences*, *34*, 237–280.
- Arend, M., & Fromm, J. (2007). Seasonal change in the drought response of wood cell development in poplar. *Tree Physiology*, *27*, 985–992.
- Arifuzzaman, M., Sayed, M. A., Muzammil, S., Pillen, K., Schumann, H., Naz, A. A., & Léon, J. (2014). Detection and validation of novel QTL for shoot and root traits in barley (*Hordeum vulgare* L.). *Molecular Breeding*, *34*(3), 1373–1387.
- Ashraf, M. (2010). Inducing drought tolerance in plants: Recent advances. *Biotechnology Advances*, *28*, 169–183.
- Awad, H., Barigah, T., Badel, E., Cochard, H., & Herbette, S. (2010). Poplar vulnerability to xylem cavitation acclimates to drier soil conditions. *Physiologia Plantarum*, *139*, 280–288.
- Bellucci, A., Tondelli, A., Fangel, J. U., Torp, A. M., Xu, X., Willats, W. G. T., et al. (2017). Genome-wide association mapping in winter barley for grain yield and culm cell wall polymer content using the high-throughput CoMPP technique. *PLoS One*, *12*(3), e0173313.
- Bernier, J., Serraj, R., Kumar, A., Venuprasad, R., Impa, S., Oane, R., ... Atlin, G. (2009). The large-effect drought-resistance QTL *qt12.1* increases water uptake in upland rice. *Field Crops Research*, *110*, 139–146.
- Blancaflor, E. B. (2013). Regulation of plant gravity sensing and signaling by the actin cytoskeleton. *American Journal of Botany*, *100*, 143–152.
- Bradbury, P. J., Zhang, Z., Kroon, D. E., Casstevens, T. M., Ramdoss, Y., & Buckler, E. S. (2007). TASSEL: Software for association mapping of complex traits in diverse samples. *Bioinformatics*, *23*, 2633–2635.
- Burton, A. L., Johnson, J., Foerster, J., Hanlon, M. T., Kaepler, S. M., Lynch, J. P., & Brown, K. M. (2015). QTL mapping and phenotypic variation of root anatomical traits in maize (*Zea mays* L.). *Theoretical and Applied Genetics*, *128*(1), 93–106.
- Burton, A. L., Williams, M., Lynch, J. P., & Brown, K. M. (2012). RootScan: Software for high-throughput analysis of root anatomical traits. *Plant and Soil*, *357*(1–2), 189–203.
- Chen, H., & Xiong, L. (2012). Genome-wide transcriptional reprogramming under drought stress. In *Plant responses to drought stress* (pp. 273–289). Berlin, Heidelberg: Springer.
- Chimungu, J. G., Brown, K. M., & Lynch, J. P. (2014). Large root cortical cell size improves drought tolerance in maize. *Plant Physiology*, *166*(4), 2166–2178.
- Chimungu, J. G., Loades, K. W., & Lynch, J. P. (2015). Root anatomical phenes predict root penetration ability and biomechanical properties in maize (*Zea mays*). *Journal of Experimental Botany*, *66*(11), 3151–3162.
- Chloupek, O., Forster, B. P., & Thomas, W. T. (2006). The effect of semi-dwarf genes on root system size in field-grown barley. *Theoretical and Applied Genetics*, *112*(5), 779–786.
- Chono, M., Honda, I., Zeniya, H., Yoneyama, K., Saisho, D., Takeda, K., et al. (2003). A semidwarf phenotype of barley uzu results from a nucleotide substitution in the gene encoding a putative brassinosteroid receptor. *Plant Physiology*, *133*(3), 1209–1219.
- Comas, L. H., Becker, S. R., Von Mark, V. C., Byrne, P. F., & Dierig, D. A. (2013). Root traits contributing to plant productivity under drought. *Frontiers in Plant Science*, *4*, 442.
- Contreras-Soto, R. I., Mora, F., de Oliveira, M. A. R., Higashi, W., Scapim, C. A., & Schuster, I. (2017). A genome-wide association study for agronomic traits in soybean using SNP markers and SNP-based haplotype analysis. *PLoS One*, *12*(2), e0171105.
- Coudert, Y., Le, V. A. T., Adam, H., Bès, M., Vignols, F., Jouannic, S., et al. (2015). Identification of CROWN ROOTLESS1-regulated genes in rice reveals specific and conserved elements of postembryonic root formation. *New Phytologist*, *206*(1), 243–254.
- Cui, X. Y., Du, Y. T., Fu, J. D., Yu, T. F., Wang, C. T., Chen, M., et al. (2018). Wheat CBL-interacting protein kinase 23 positively regulates drought stress and ABA responses. *BMC Plant Biology*, *18*(1), 93.
- de Koning, D. J., & Haley, C. S. (2005). Genetical genomics in humans and model organisms. *Trends in Genetics*, *21*(7), 377–381.
- De Smet, I., Signora, L., Beeckman, T., Inze, D., Foyer, C. H., & Zhang, H. (2003). An abscisic acid-sensitive checkpoint in lateral root development of Arabidopsis. *The Plant Journal*, *33*, 543–555.
- Diab, A. A., Teulat-Merah, B., This, D., Ozturk, N. Z., Benschel, D., & Sorrells, M. E. (2004). Identification of drought-inducible genes and differentially expressed sequence tags in barley. *Theoretical and Applied Genetics*, *109*(7), 1417–1425.
- Ehdaie, B., Layne, A. P., & Waines, J. G. (2012). Root system plasticity to drought influences grain yield in bread wheat. *Euphytica*, *186*, 219–232.
- Eissenstat, D. M. (1992). Costs and benefits of constructing roots of small diameter. *Journal of Plant Nutrition*, *15*, 763–782.
- Evanno, G., Regnaut, S., & Goudet, J. (2005). Detecting the number of clusters of individuals using the software STRUCTURE: A simulation study. *Molecular Ecology*, *14*, 2611–2620.
- Fang, C., Ma, Y., Wu, S., Liu, Z., Wang, Z., Yang, R., et al. (2017). Genome-wide association studies dissect the genetic networks underlying agronomical traits in soybean. *Genome Biology*, *18*(1), 161.
- Farooq, M., Basra, S. M. A., Wahid, A., Ahmad, N., & Saleem, B. A. (2009). Improving the drought tolerance in rice (*Oryza sativa* L.) by exogenous application of salicylic acid. *Journal of Agronomy and Crop Science*, *195*, 237–246.
- Farooq, M., Wahid, A., Cheema, S. A., Lee, D. J., & Aziz, T. (2010). Comparative time course action of the foliar applied glycinebetaine, salicylic acid, nitrous oxide, brassinosteroids and spermine in improving drought resistance of rice. *Journal of Agronomy and Crop Science*, *196*, 336–345.
- Fernandez, G. C. J. (1992). Effective selection criteria for assessing plant stress tolerance. *Adaptation of vegetable and other food crops in temperature and water stress: proceedings of an international symposium, Taiwan, 13–16 August 1992* (pp. 257–270). Taipei: Asian Vegetable Research and Development Center.
- Fujita, M., Fujita, Y., Noutoshi, Y., Takahashi, F., Narusaka, Y., Yamaguchi-Shinozaki, K., & Shinozaki, K. (2006). Crosstalk between abiotic and biotic stress responses: A current view from the points of convergence in the stress signaling networks. *Current Opinion in Plant Biology*, *9*, 436–442.

- Gao, Y., & Lynch, J. P. (2016). Reduced crown root number improves water acquisition under water deficit stress in maize (*Zea mays* L.). *Journal of Experimental Botany*, 67(15), 4545–4557.
- Ge, B., Pokholok, D. K., Kwan, T., Grundberg, E., Morcos, L., Verlaan, D. J., et al. (2009). Global patterns of cis variation in human cells revealed by high-density allelic expression analysis. *Nature Genetics*, 41(11), 1216.
- Geng, D., Chen, P., Shen, X., Zhang, Y., Li, X., Jiang, L., et al. (2018). MdMYB88 and MdMYB124 enhance drought tolerance by modulating root vessels and cell walls in apple. *Plant Physiology*, 178(3), 1296–1309.
- GenStat. (2014) VSN. GenStat for Windows, 16th edn. VSN International Hemel Hempstead, UK.
- Gilmour, A. R., Thompson, R., & Cullis, B. R. (1995). Average information REML: An efficient algorithm for variance parameters estimation in linear mixed models. *Biometrics*, 51, 1440–1450.
- Gous, P. W., Hickey, L., Christopher, J. T., Franckowiak, J., & Fox, G. P. (2016). Discovery of QTL for stay-green and heat-stress in barley (*Hordeum vulgare*) grown under simulated abiotic stress conditions. *Euphytica*, 207(2), 305–317.
- Gudys, K., Guzy-Wrobelska, J., Janiak, A., Dziurka, M. A., Ostrowska, A., Hura, K., et al. (2018). Prioritization of candidate genes in QTL regions for physiological and biochemical traits underlying drought response in barley (*Hordeum vulgare* L.). *Frontiers in Plant Science*, 9, 769.
- Guo, Y., Jiang, Q., Hu, Z., Sun, X., Fan, S., & Zhang, H. (2018). Function of the auxin-responsive gene TaSAUR75 under salt and drought stress. *The Crop Journal*, 6(2), 181–190.
- Habte, E., Müller, L. M., Shtaya, M., Davis, S. J., & Korff, M. (2014). Osmotic stress at the barley root affects expression of circadian clock genes in the shoot. *Plant, Cell & Environment*, 37(6), 1321–1337.
- Hagen, G., & Guilfoyle, T. (2002). Auxin-responsive gene expression: Genes, promoters and regulatory factors. *Plant Molecular Biology*, 49(3–4), 373–385.
- Hall, B., & Lanba, A. (2019). Three-dimensional analysis of biological systems via a novel laser ablation technique. *Journal of Laser Applications*, 31(2), 022602.
- Hamblin, M. T., Close, T. J., Bhat, P. R., Chao, S. M., Kling, J. G., et al. (2010). Population structure and linkage disequilibrium in US barley germplasm: Implications for association mapping. *Crop Science*, 50, 556–566.
- Hose, E., Clarkson, D. T., Steudle, E., & Hartung, W. (2001). The exodermis: A variable apoplastic barrier. *Journal of Experimental Botany*, 52, 2254–2264.
- IBGC. (2012). International Barley Genome Sequencing Consortium: A physical, genetic and functional sequence assembly of the barley genome. *Nature*, 491(7426), 711.
- Janiak, A., Kwaśniewski, M., & Szarejko, I. (2015). Gene expression regulation in roots under drought. *Journal of Experimental Botany*, 67(4), 1003–1014.
- Jannink, J. L., Moreau, L., Charmet, G., & Charcosset, A. (2009). Overview of QTL detection in plants and tests for synergistic epistatic interactions. *Genetica*, 136, 225–236.
- Jannink, J. L., & Wu, X. L. (2003). Estimating allelic number and identity in state of QTLs in interconnected families. *Genet. Res.*, 2003(81), 133–144.
- Jarzyniak, K. M., & Jasinski, M. (2014). Membrane transporters and drought resistance - a complex issue. *Frontiers in Plant Science*, 5, 687.
- Jia, Z., Liu, Y., Gruber, B. D., Neumann, K., Kilian, B., Graner, A., & Von Wirén, N. (2019). Genetic dissection of root system architectural traits in spring barley. *Frontiers in Plant Science*, 10, 400.
- Jighly, A., Oyiga, B. C., Makdis, F., Nazari, K., Youssef, O., Tadesse, W., et al. (2015). Genome-wide DArT and SNP scan for QTL associated with resistance to stripe rust (*Puccinia striiformis* f. sp. tritici) in elite ICARDA wheat (*Triticum aestivum* L.) germplasm. *Theoretical and Applied Genetics*, 128(7), 1277–1295.
- Jovanovic, M., Rielefebvre, V., Laporte, P., Gonzales-Rizzo, S., Lelandais-Brière, C., Frugier, F., ... Crespi, M. (2007). How the environment regulates root architecture in dicots. *Advances in Botanical Research*, 46, 35–74.
- Kadam, N., Tamilselvan, A., Lawas, L. M. F., Quinones, C., Bahuguna, R., Thomson, M. J., et al. (2017). Genetic control of plasticity in root morphology and anatomy of rice in response to water-deficit. *Plant Physiology*, 174, 2302–2315.
- Kadam, N. N., Yin, X., Bindrabab, P. S., Struik, P. C., & Jagadish, K. S. V. (2015). Does morphological and anatomical plasticity during the vegetative stage make wheat more tolerant of water deficit stress than rice? *Plant Physiology*, 167(4), 1389–1401.
- Kang H.M., Sul J.H., Service S.K., Zaitlen N.A., Kong S.Y., et al. (2010). Variance component model to account for sample structure in genome-wide association studies. *Nature Genetics*, 42, 348–354.
- Kaur, G., Singh, S., Dutta, T., Kaur, H., Singh, B., Pareek, A., & Singh, P. (2016). The peptidyl-prolyl cis-trans isomerase activity of the wheat cyclophilin, TaCypA-1, is essential for inducing thermos-tolerance in *Escherichia coli*. *Biochimie Open*, 2, 9–15.
- Khan, M. A., Gemenet, D. C., & Villordon, A. (2016). Root system architecture and abiotic stress tolerance: Current knowledge in root and tuber crops. *Frontiers in Plant Science*, 7, 1584.
- Krzywinski, M., et al. (2009). Circo: An information aesthetic for comparative genomics. *Genome Research*, 19, 1639–1645.
- Ksouri, N., Jiménez, S., Wells, C. E., Contreras-Moreira, B., & Gogorcena, Y. (2016). Transcriptional responses in root and leaf of *Prunus persica* under drought stress using RNA sequencing. *Frontiers in Plant Science*, 7, 1715.
- Kuhlmann, H., & Barraclough, P. B. (1987). Comparison between the seminal and nodal root systems of winter wheat in their activity for N and K uptake. *Zeitschrift für Pflanzenernährung und Bodenkunde*, 150(1), 24–30.
- Kulkarni, M., Soolanayakanahally, R., Ogawa, S., Uga, Y., Selvaraj, M. G., & Kagale, S. (2017). Drought response in wheat: Key genes and regulatory mechanisms controlling root system architecture and transpiration efficiency. *Frontiers in Chemistry*, 5, 106.
- Lo Gullo, M. A., Nardini, A., Salleo, S., & Tyree, M. T. (1998). Changes in root hydraulic conductance of *Olea oleaster* seedlings following drought stress and irrigation. *New Phytologist*, 140, 25–31.
- Lynch, J. (1995). Root architecture and plant productivity. *Plant Physiology*, 109, 7–13.
- Lynch, J. (2013). Steep, cheap and deep: An ideotype to optimize water and n acquisition by maize root systems. *Annals of Botany*, 2(11), 347–357.
- Lynch, J. P., & Beebe, S. E. (1995). Adaptation of beans (*Phaseolus vulgaris* L.) to low phosphorus availability. *HortScience*, 30, 1165–1171.
- Lynch, J. P., & Brown, K. M. (2012). New roots for agriculture: Exploiting the root phenome. *Philosophical Transactions of the Royal Society of London B: Biological Sciences*, 367, 1598–1604.
- Lynch, J. P., Chimungu, J. G., & Brown, K. M. (2014). Root anatomical phenes associated with water acquisition from drying soil: Targets for crop improvement. *Journal of Experimental Botany*, 65, 6155–6166.
- Lynch, J. P., & Wojciechowski, T. (2015). Opportunities and challenges in the subsoil: Pathways to deeper rooted crops. *Journal of Experimental Botany*, 66(8), 2199–2210.
- Lynch, J. P. (2007). Roots of the second green revolution. *Australian Journal of Botany*, 55, 493–512.
- Lynch, J. P. (2014). Root phenes that reduce the metabolic costs of soil exploration: Opportunities for 21st century agriculture. *Plant, Cell & Environment*, 38(9), 1775–1784. <https://doi.org/10.1111/pce.12451>
- Manavalan, L. P., Musket, T., & Nguyen, H. T. (2012). Natural genetic variation for root traits among diversity lines of maize (*Zea mays* L.). *Maydica*, 56(1), 59–68.
- Mascher, M., Gundlach, H., Himmelbach, A., Beier, S., Twardziok, S. O., Wicker, T., et al. (2017). A chromosome conformation capture ordered sequence of the barley genome. *Nature*, 544(7651), 427.
- Merchuk-Ovnat, L., Fahima, T., Ephrath, J. E., Krugman, T., & Saranga, Y. (2017). Ancestral QTL alleles from wild emmer wheat enhance root

- development under drought in modern wheat. *Frontiers in Plant Science*, 8, 703.
- Mezaka, I., Legzdina, L., Waugh, R., Close, T., & Rostoks, N. (2013). Genetic diversity in Latvian spring barley association mapping population. In G. Zhang, C. Li, & X. Liu (Eds.), *Advance in barley sciences* (pp. 25–35). Dordrecht: Springer.
- Mohammadi, R., Armionb, M., Kahrizic, D., & Amri, A. (2010). Efficiency of screening techniques for evaluating durum wheat genotypes under mild drought conditions. *International Journal of Plant Production*, 4(1), 11–24.
- Nelson, D. C., Flematti, G. R., Riseborough, J. A., Ghisalberti, E. L., Dixon, K. W., & Smith, S. M. (2010). Karrikins enhance light responses during germination and seedling development in *Arabidopsis thaliana*. *Proceedings of the National Academy of Sciences*, 107(15), 7095–7100.
- Nestler, J., Liu, S., Wen, T. J., Paschold, A., Marcon, C., Tang, H. M., et al. (2014). Roothairless5, which functions in maize (*Zea mays* L.) root hair initiation and elongation encodes a monocot-specific NADPH oxidase. *The Plant Journal*, 79(5), 729–740.
- North, G. B., & Nobel, P. S. (1992). Drought-induced changes in hydraulic conductivity and structure in roots of *Ferocactus acanthodes* and *Opuntia ficus-indica*. *New Phytologist*, 120, 9–19.
- O'Neill, M. (2010). ANOVA and REML: A guide to linear mixed models in an experimental design context, statistical advisory and training service Pty Ltd, 180 pp.
- Ogbonnaya, F. C., Rasheed, A., Okechukwu, E. C., Jighly, A., Makdis, F., et al. (2017). Genome-wide association study for agronomic and physiological traits in spring wheat evaluated in a range of heat prone environments. *Theoretical and Applied Genetics*, 130(9), 1819–1835.
- Oyiga, B. C., Ogbonnaya, F. C., Sharma, R. C., Baum, M., Léon, J., & Ballvora, A. (2019). Genetic and transcriptional variations in NRAMP-2 and OPAQUE1 genes are associated with salt stress response in wheat. *Theoretical and Applied Genetics*, 132(2), 323–346.
- Oyiga, B. C., Sharma, R. C., Baum, M., Ogbonnaya, F. C., Léon, J., & Ballvora, A. (2018). Allelic variations and differential expressions detected at quantitative trait loci for salt stress tolerance in wheat. *Plant, Cell & Environment*, 41(5), 919–935.
- Pacheco-Villalobos, D., & Hardtke, C. S. (2012). Natural genetic variation of root system architecture from *Arabidopsis* to *Brachypodium*: Towards adaptive value. *Philosophical Transactions of the Royal Society of London B: Biological Sciences*, 367(1595), 1552–1558.
- Paez-Garcia, A., Motes, C., Scheible, W. R., Chen, R., Blancaflor, E., & Monteros, M. (2015). Root traits and phenotyping strategies for plant improvement. *Plants*, 4(2), 334–355.
- Palta, J. A., & Yang, J. C. (2014). Crop root system behaviour and yield preface. *Field Crops Research*, 165, 1–4.
- Pasam, R. K., Sharma, R., Malosetti, M., van Eeuwijk, F. A., Haseneyer, G., Kilian, B., & Graner, A. (2012). Genome-wide association studies for agronomical traits in a world wide spring barley collection. *BMC Plant Biology*, 12, 16.
- Peakall, R., & Smouse, P. E. (2012). GenAEx 6.5: Genetic analysis in Excel. Population genetic software for teaching and research—an update. *Bioinformatics*, 28, 2537–2539.
- Peña-Valdivia, C. B., & Sánchez-Urdaneta, A. B. (2009). Effects of substrate water potential in root growth of *Agave salmiana* Otto ex Salm-Dyck seedlings. *Biological Research*, 42, 239–248.
- Pillen, K., Zacharias, A., & Leon, J. (2003). Advanced backcross QTL analysis in barley (*Hordeum vulgare* L.). *Theoretical and Applied Genetics*, 107(2), 340–352.
- Polanía Perdomo, J. A., Rao, I. M., Cajiao, V., Hernando, C., Grajales, M. A., Rivera, M., et al. (2017). Shoot and root traits contribute to drought resistance in recombinant inbred lines of MD 23–24× SEA 5 of common bean. *Frontiers in Plant Science*, 8, 296.
- Postma, J. A., & Lynch, J. P. (2011). Root cortical aerenchyma enhances the growth of maize on soils with suboptimal availability of nitrogen, phosphorus, and potassium. *Plant Physiology*, 156, 1190–1201.
- Price, A. L., Zaitlen, N. A., Reich, D., & Patterson, N. (2010). New approaches to population stratification in genome-wide association studies. *Nature Reviews Genetics*, 11, 459–463.
- Pritchard, J. K., Stephens, M., & Donnelly, P. (2000). Inference of population structure using multilocus genotype data. *Genetics*, 155, 945–959.
- Ram, M. (2014). *Plant Breeding Methods*. Asoke K. Ghosh, PHI Learning Pvt. Ltd.
- Raman, H., Wang, J. P., Read, B., Zhou, M. X., Venkataganappa, S., Moroni, J. S., et al. (2005). Molecular mapping of resistance to aluminium toxicity in barley. In Proceedings of Plant and Animal Genome XIII Conference, January (pp. 15–19).
- Remy, E., Cabrito, T. R., Baster, P., Batista, R. A., Teixeira, M. C., Friml, J., et al. (2013). A major facilitator superfamily transporter plays a dual role in polar auxin transport and drought stress tolerance in *Arabidopsis*. *The Plant Cell*, 25(3), 901–926.
- Richards, R. A., & Passioura, J. B. (1989). A breeding program to reduce the diameter of the major xylem vessel in the seminal roots of wheat and its effect on grain yield in rain-fed environments. *Australian Journal of Agricultural Research*, 40(5), 943–950.
- Ristova, D., Metesch, K., & Busch, W. (2017). Natural genetic variation shapes root system responses to phytohormones in *Arabidopsis*. *The Plant Journal*, 96(2), 468–481.
- Rosas, U., Cibrián-Jaramillo, A., Ristova, D., Banta, J. A., Gifford, M. L., Fan, A. H., et al. (2013). Integration of responses within and across *Arabidopsis* natural accessions uncovers loci controlling root systems architecture. *Proceedings of the National Academy of Sciences*, 110(37), 15133–15138.
- Rostamza, M., Richards, R. A., & Watt, M. (2013). Response of millet and sorghum to a varying water supply around the primary and nodal roots. *Annals of Botany*, 112, 439–446.
- Ruggiero, A., Punzo, P., Landi, S., Costa, A., Van Oosten, M., & Grillo, S. (2017). Improving plant water use efficiency through molecular genetics. *Horticulturae*, 3(2), 31.
- Sadok, W., & Sinclair, T. R. (2011). Crops yield increase under water-limited conditions: Review of recent physiological advances for soybean genetic improvement. *Advances in agronomy*, 113, 313–337.
- Saengwilai, P., Tian, X., & Lynch, J. P. (2014). Low crown root number enhances nitrogen acquisition from low-nitrogen soils in maize. *Plant Physiology*, 166, 581–589.
- Sato, E. M., Hijazi, H., Bennett, M. J., Vissenberg, K., & Swarup, R. (2014). New insights into root gravitropic signalling. *Journal of Experimental Botany*, 66(8), 2155–2165. <https://doi.org/10.1093/jxb/eru515>
- Sebastian, J., Yee, M. C., Goudinho Viana, W., Rellán-Álvarez, R., Feldman, M., Priest, H. D., et al. (2016). Grasses suppress shoot-borne roots to conserve water during drought. *Proceedings of the National Academy of Sciences of the United States of America*, 113, 8861–8866.
- Shida, T., Fukuda, A., Saito, T., Ito, H., & Kato, A. (2015). AtRBP1, which encodes an RNA-binding protein containing RNA-recognition motifs, regulates root growth in *Arabidopsis thaliana*. *Plant Physiology and Biochemistry*, 92, 62–70.
- Shin, H., Shin, H. S., Guo, Z., Blancaflor, E. B., Masson, P. H., & Chen, R. (2005). Complex regulation of *Arabidopsis* AGR1/PIN2-mediated root gravitropic response and basipetal auxin transport by cantharidin-sensitive protein phosphatases. *The Plant Journal*, 42, 188–200.
- Sio-Se, M. A., Ahmadi, A., Poustini, K., & Mohammadi, V. (2006). Evaluation of drought resistance indices under various environmental conditions. *Field Crops Research*, 98, 222–229.
- Smith, S., & De Smet, I. (2012). Root system architecture: Insights from *Arabidopsis* and cereal crops. *Philosophical Transactions of the Royal Society of London B: Biological Sciences*, 367, 1441–1452.
- Steele, K., Virk, D., Kumar, R., Prasad, S., & Witcombe, J. (2007). Field evaluation of upland rice lines selected for QTLs controlling root traits. *Field Crops Research*, 101, 180–186.

- Stein, N., Herren, G., & Keller, B. (2001). A new DNA extraction method for high-throughput marker analysis in a large-genome species such as *Triticum aestivum*. *Plant Breeding*, 120(4), 354–356.
- Storey, J. D., & Tibshirani, R. (2003). Statistical significance for genome-wide experiments. *Proceeding of the National Academy of Sciences*, 100, 9440–9445.
- Strock, C. F., De La Riva, L. M., & Lynch, J. P. (2018). Reduction in root secondary growth as a strategy for phosphorus acquisition. *Plant Physiology*, 176(1), 691–703.
- Strock, C. F., Schneider, H. M., Galindo-Castañeda, T., Hall, B. T., Van Gansbeke, B., Mather, D. E., ... Lynch, J. P. (2019). Laser ablation tomography for visualization of root colonization by edaphic organisms. *Journal of Experimental Botany*, 70(19), 5327–5342. <https://doi.org/10.1093/jxb/erz271>
- Szalai, G., Horgosi, S., Soos, V., Majlath, I., Balazs, E., & Janda, T. (2010). Salicylic acid treatment of pea seeds induces its de novo synthesis. *Journal of Plant Physiology*, 168, 213–219.
- Takanashi, K., Shitan, N., & Yazaki, K. (2014). The multidrug and toxic compound extrusion (MATE) family in plants. *Plant Biotechnology*, 31, 417–430.
- Teulat, B., Borries, C., & This, D. (2001). New QTLs identified for plant water status, water-soluble carbohydrate and osmotic adjustment in a barley population grown in a growth-chamber under two water regimes. *Theoretical and Applied Genetics*, 103(1), 161–170.
- Thoen, M. P., Davila Olivas, N. H., Kloth, K. J., Coolen, S., Huang, P. P., Aarts, M. G., et al. (2017). Genetic architecture of plant stress resistance: Multi-trait genome-wide association mapping. *New Phytologist*, 213(3), 1346–1362.
- Topp, C. N., Iyer-Pascuzzi, A. S., Anderson, J. T., Lee, C. R., Zurek, P. R., Symonova, O., et al. (2013). 3D phenotyping and quantitative trait locus mapping identify core regions of the rice genome controlling root architecture. *Proceedings of the National Academy of Sciences*, 110(18), E1695–E1704.
- Trachsel, S., Kaeppeler, S. M., Brown, K. M., & Lynch, J. P. (2011). Shovelomics: High throughput phenotyping of maize root architecture in the field. *Plant Soil*, 341, 75–87.
- Tron, S., Bodner, G., Laio, F., Ridolfi, L., & Leitner, D. (2015). Can diversity in root architecture explain plant water use efficiency? A modeling study. *Ecological Modelling*, 312, 200–210.
- Tuberosa, R., Salvi, S., Sanguineti, M. C., Maccaferri, M., Giuliani, S., & Landi, P. (2003). Searching for QTLs controlling root traits in maize: A critical appraisal. *Plant Soil*, 255, 35–54.
- Uga, Y., Sugimoto, K., Ogawa, S., Rane, J., Ishitani, M., Hara, N., et al. (2013). Control of root system architecture by DEEPER ROOTING 1 increases rice yield under drought conditions. *Nature Genetics*, 45, 1097–1102.
- Ulmasov, T., Hagen, G., & Guilfoyle, T. J. (1997). ARF1, a transcription factor that binds to auxin response elements. *Science*, 276, 1865–1868.
- Ulmasov, T., Hagen, G., & Guilfoyle, T. J. (1999). Dimerization and DNA binding of auxin response factors. *Plant Journal*, 19, 309–319.
- Vasseur, F., Exposito-Alonso, M., Ayala-Garay, O. J., Wang, G., Enquist, B. J., Vile, D., et al. (2018). Adaptive diversification of growth allometry in the plant *Arabidopsis thaliana*. *Proceedings of the National Academy of Sciences*, 115(13), 3416–3421.
- van der Sijde, M. R., Ng, A., & Fu, J. (2014). Systems genetics: From GWAS to disease pathways. *Biochimica et Biophysica Acta (BBA)-Molecular Basis of Disease*, 1842(10), 1903–1909.
- Von Korff, M., Grando, S., Del Greco, A., This, D., Baum, M., & Ceccarelli, S. (2008). Quantitative trait loci associated with adaptation to Mediterranean dryland conditions in barley. *Theoretical and Applied Genetics*, 117(5), 653–669.
- Wang, C., Lu, W., He, X., Wang, F., Zhou, Y., Guo, X., & Guo, X. (2016). The cotton mitogen-activated protein kinase 3 functions in drought tolerance by regulating stomatal responses and root growth. *Plant and Cell Physiology*, 57(8), 1629–1642.
- Wasson, A. P., Richards, R. A., Chatrath, R., Misra, S. C., Prasad, S. S., Rebetzke, G. J., et al. (2012). Traits and selection strategies to improve root systems and water uptake in water-limited wheat crops. *Journal of Experimental Botany*, 63, 3485–3498.
- Wei, Z., & Li, J. (2018). Receptor-like protein kinases: Key regulators controlling root hair development in *Arabidopsis thaliana*. *Journal of Integrative Plant Biology*, 60(9), 841–850.
- Wójcik-Jagła, M., Fiust, A., Kościelniak, J., & Rapacz, M. (2018). Association mapping of drought tolerance-related traits in barley to complement a traditional bi-parental QTL mapping study. *Theoretical and Applied Genetics*, 131(1), 167–181.
- Wójcik-Jagła, M., Rapacz, M., Tyrka, M., Kościelniak, J., Crissy, K., & Żmuda, K. (2013). Comparative QTL analysis of early short-time drought tolerance in Polish fodder and malting spring barleys. *Theoretical and Applied Genetics*, 126(12), 3021–3034.
- Xi, W., Gong, X., Yang, Q., Yu, H., & Liou, Y. C. (2016). Pin1At regulates PIN1 polar localization and root gravitropism. *Nature Communications*, 7, 10430.
- Xiong, L., Wang, R. G., Mao, G., & Koczan, J. M. (2006). Identification of drought tolerance determinants by genetic analysis of root response to drought stress and abscisic acid. *Plant Physiology*, 142(3), 1065–1074.
- Xiong, Y. C., Li, F. M., & Zhang, T. (2006). Performance of wheat crops with different chromosome ploidy: Root-sourced signals, drought tolerance, and yield performance. *Planta*, 224(3), 710–718.
- York, L. M., Galindo-Castaneda, T., Schussler, J. R., & Lynch, J. P. (2015). Evolution of US maize (*Zea mays* L.) root architectural and anatomical phenes over the past 100 years corresponds to increased tolerance of nitrogen stress. *Journal of Experimental Botany*, 66(8), 2347–2358. <https://doi.org/10.1093/jxb/erv074>
- Yu, G., Pressoir, W. H., Briggs, I. V., Bi, M., Yamasaki, J. F., Doebley, M. D., et al. (2006). A unified mixed-model method for association mapping that accounts for multiple levels of relatedness. *Nature Genetics*, 38(2), 203–208.
- Zaidi P.H., Seetharam K., Krishna G., Krishnamurthy L., Gajanan S., Babu R., et al. (2016). Genomic regions associated with root traits under drought stress in tropical maize (*Zea mays* L.). *PLoS One*, 11(10), e0164340. <https://doi.org/10.1371/journal.pone.0164340>
- Zaman-Allah, M., Jenkinson, D. M., & Vadez, V. (2011). Chickpea genotypes contrasting for seed yield under terminal drought stress in the field differ for traits related to the control of water use. *Functional Plant Biology*, 38, 270–281.
- Zhan, A., Schneider, H., & Lynch, J. (2015). Reduced lateral root branching density improves drought tolerance in maize. *Plant Physiology*, 168(4), 1603–1615.
- Zhang, H., Zhu, H., Pan, Y., Yu, Y., Luan, S., & Li, L. (2014). A DTX/MATE-type transporter facilitates abscisic acid efflux and modulates ABA sensitivity and drought tolerance in *Arabidopsis*. *Molecular Plant*, 7(10), 1522–1532.
- Zhou, X., Li, Q., Chen, X., Liu, J., Zhang, Q., Liu, Y., et al. (2011). The *Arabidopsis* RETARDED ROOT GROWTH gene encodes a mitochondria-localized protein that is required for cell division in the root meristem. *Plant Physiology*, 157(4), 1793–1804.
- Zhu, J., Brown, K. M., & Lynch, J. P. (2010). Root cortical aerenchyma improves the drought tolerance of maize (*Zea mays* L.). *Plant, Cell & Environment*, 33(5), 740–749.

SUPPORTING INFORMATION

Additional supporting information may be found online in the Supporting Information section at the end of this article.

How to cite this article: Oyiga BC, Palczak J, Wojciechowski T, et al. Genetic components of root architecture and anatomy adjustments to water-deficit stress in spring barley. *Plant Cell Environ*. 2019;1–20. <https://doi.org/10.1002/pce.13683>